CZECH ACADEMY OF AGRICULTURAL SCIENCES

Research in AGRICULTURAL ENGINEERING

ZEMĚDĚLSKÁ TECHNIKA

INSTITUTE OF AGRICULTURAL AND FOOD INFORMATION

4

VOLUME 48
PRAGUE 2002
ISSN 1212-9151

RESEARCH IN AGRICULTURAL ENGINEERING

formerly ZEMĚDĚLSKÁ TECHNIKA since 1954 to 1999

An international journal published under the auspices of the Czech Academy of Agricultural Sciences and financed by the Ministry of Agriculture of the Czech Republic

Mezinárodní vědecký časopis vydávaný pod záštitou České akademie zemědělských věd a s finanční podporou Ministerstva zemědělství České republiky

---

Aims and scope: The journal publishes original scientific papers and review studies on agricultural engineering, agricultural technology, processing of agricultural products, countryside buildings and related problems from ecology, energetics, economy, ergonomy and applied physics and chemistry. Abstracts from the journal are comprised in the databases: Agris, CAB Abstracts, Czech Agricultural Bibliography.

Periodicity: The journal is published quarterly (4 issues per year). Volume *48* is appearing in 2002.

Submission of manuscripts: Two copies of manuscript should be addressed to: Mgr. Radka Chlebečková, editor-in-chief, Institute of Agricultural and Food Information, Slezská 7, 120 56 Prague 2, Czech Republic, tel.: + 420 2 27 01 03 55, fax: + 420 2 27 01 01 16, e-mail: forest@uzpi.cz. The day the manuscript reaches the editor for the first time is given upon publication as the date of receipt.

Subscription information: Subscription orders can be entered only by calendar year and should be sent to the above address. Subscription price is 92 USD (Europe) and 97 USD (overseas).

Cíl a odborná náplň: Časopis publikuje původní vědecké práce a studie typu review z oborů zemědělská technika, zemědělské technologie, zpracování zemědělských produktů, venkovské stavby a s tím spojených problémů ekologických, energetických, ekonomických, ergonomických a agrofyzikálních. Abstrakty z časopisu jsou zahrnuty v těchto databázích: Agris, CAB Abstracts, Czech Agricultural Bibliography.

Periodicita: Časopis vychází čtvrtletně (4krát ročně). Ročník *48* vychází v roce 2002.

Přijímání rukopisů: Rukopisy ve dvou kopiích je třeba zaslat na adresu: Mgr. Radka Chlebečková, vedoucí redaktorka, Ústav zemědělských a potravinářských informací, Slezská 7, 120 56 Praha 2, Česká republika, tel.: + 420 2 27 01 03 55, fax: + 420 2 27 01 01 16, e-mail: forest@uzpi.cz. Den doručení rukopisu do redakce je uveřejněn jako datum přijetí k publikaci.

Informace o předplatném: Objednávky na předplatné jsou přijímány na celý rok na adrese: Ústav zemědělských a potravinářských informací, Slezská 7, 120 56 Praha 2. Cena předplatného pro rok 2002 je 352 Kč.

Up-to-date information are available at address **http://www.cazv.cz**

Aktuální informace najdete na URL adrese **http://www.cazv.cz**

MK ČR E 6698

Device for measuring the forces influencing duckfoot shares

M. FRÍD, J. ŠABATKA

University of South Bohemia, Faculty of Agriculture, České Budějovice

ABSTRACT: The purpose of this Research project – CEZ: J06/98 122200002/I – was to design, construct and test the device MV-97. This equipment makes possible the measurement of forces that affect the symmetric working parts of soil cultivators both in the vertical and horizontal planes. The design of mechanical implements comes both from the theoretical analysis of forces affecting one-hinge suspension and from conditions for the equilibrium of such forces. The electronic elements of this device, comprising software and a computer, record and save the sequence of the measured values.

Keywords: duckfoot shares; recording of forces; one-hinge suspension; dynamometers; computer

Soil processing in plant production is a very important factor influencing the yield of a harvest. Also soil processing, not done in the right way and on time, reduces the stability of yields and soil fertility. The main factor in soil processing is the clearing away of weeds, parasites and other diseases. Crucial also is the influence of soil processing in the economical use of soil moisture. When producing huge amounts of crops, inappropriate rainfall could have the main impact on yields. That is why we focus on the best results in reducing costs, lowering fuel consumption, time, working forces and soil consolidation. ANKEN et al. (1993) explain the requirements for studying the function of modern cultivators. Similar conclusions were drawn by JÄGER and FUNK (1994). HŮLA and MAYER (1995) came to the same conclusions. They also examined in detail the factors that influence the resistance of the working elements of the shovel cultivator. It is very important to know the exact weight and direction of forces over time F_x and $F_z = f(t)$, because of finding out the impact of each factor on the need for energy during soil processing.

MATERIAL AND METHODS

Either the working parts of weeders or whole working sections have to be connected with a frame in order to follow the field's surface independently and to achieve a constant depth of soil processing. This can be achieved thanks to the four-hinge mechanism (parallelogram or lever system). When designing the measuring equipment we took into account constructional solutions of one-hinge suspension with supporting wheel and the

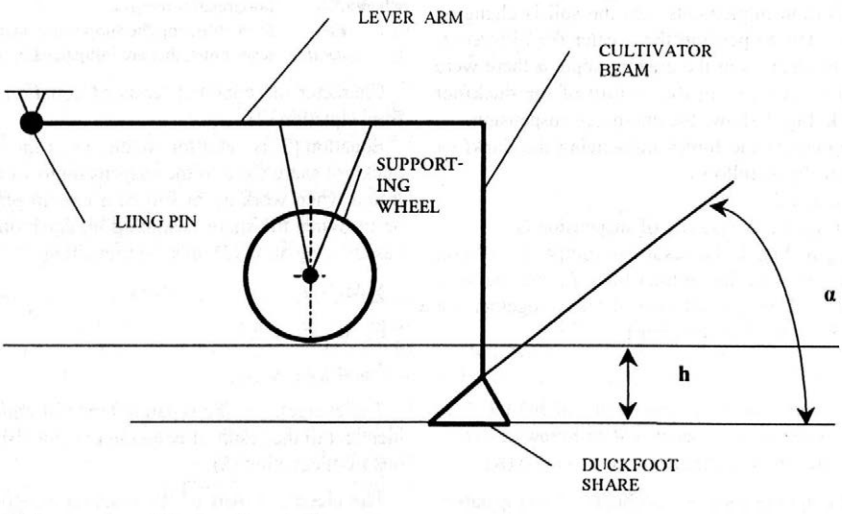

Fig. 1. One-point suspension with supporting wheel

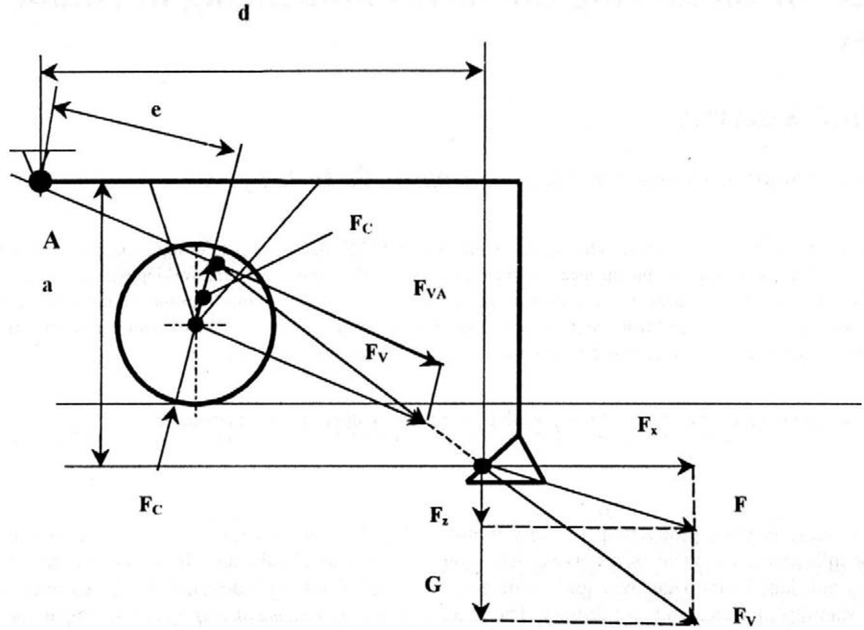

Fig. 2. Forces influencing one-point suspension with supporting wheel

theoretical analysis of forces and moments influencing the suspension.

One-hinge suspension consists of a double lever arm that is fastened to swing freely in front of a horizontal hinge on the supporting frame console. The cultivator beam that is used for assembling the working implements is fixed to the second part of the lever arm. In front of the working tool is a wheel or a sole that is designed to measure the ruggedness of the land's surface. When copying the surface, the angle (**α**) of insertion of the cultivation implements into the soil is changing – the shorter the suspension the greater the difference. According to changes in the grazing angle **α** there were corresponding changes in the quality of the duckfoot share's work. Fig. 1 shows the one-hinge suspension.

Fig. 2 represents the forces influencing the duckfoot share graphically as follows:

1. Soil resistance *F*.
2. Force expressing the gravity of suspension *G*.

According to Fig. 2 the resulting component of soil resistance consists of the vertical force F_x and the horizontal force F_z. If we put all vertical forces together, we will obtain the force F_T (equation 1).

$$F_T = F_z + G \qquad \text{(N)} \qquad (1)$$

where: F_z – force showing the gravity of soil and the force needed for the separation of the furrow slice (N),
G – force showing the gravity of suspension (N).

The total outgoing force F_V is obtained from equation (2):

$$F_V = \sqrt{F_T + F_x} \qquad \text{(N)} \qquad (2)$$

For the equilibrium of forces influencing the duckfoot share, which is fixed to the one-hinge suspension, equation (3), which expresses the equilibrium of moments.

$$\sum M_A = 0 \qquad \text{(N.m)} \qquad (3)$$

$$F_T \,.\, d - F_x \,.\, a - F_C \,.\, e = 0$$

where: F_T – sum of vertical forces (N).

$$F_T \,.\, d = F_x \,.\, a + F_C \,.\, e$$

where: F_x – horizontal force (N),
F_C – force affecting the supporting wheel (N),
a,e,d – lever arms, that are influenced by forces (m).

Character of separated terms of equation is obvious from equation (2).

Equation (3) is valid for conditions of the work of the duckfoot share fixed to the suspension to working depth ***h*** and when working in soil of a certain physical property. When the share is sinking in, equation (4) that is based on equation (3) must be prevailing.

$$\sum M_A \geq 0 \qquad \text{(N.m)} \qquad (4)$$

$$F_T \,.\, d - F_x \,.\, a \geq 0$$

$$F_T \,.\, d \geq F_x \,.\, a$$

The character of the separate terms of equation (4) is identical to the result of equation (3) and also it is obvious from equation (2).

The electronic part of the machinery equipped with software and computer, makes up the self-standing part

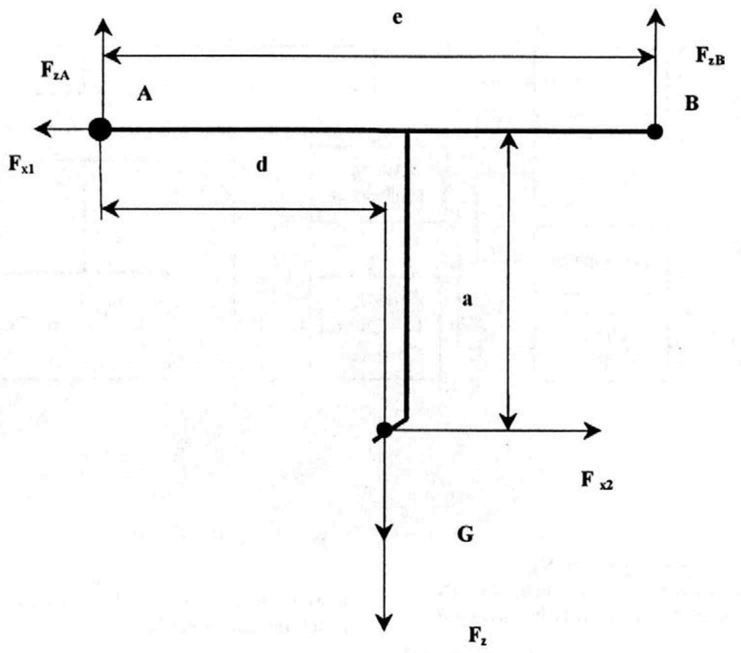

Fig. 3. Forces influencing the suspension MV-97

of the measuring equipment, which was constructed with PaedDr. Petr Adámek, Ph.D., at Faculty of Agriculture University of South Bohemia České Budějovice.

RESULTS AND DISCUSSION

a) Theoretical analysis of forces and moments influencing the suspension of measuring equipment MV-97

The analysis of forces influencing the modified suspension comes from BRZKOVSKÝ (1965) solution of the duckfoot share with supporting wheel. The idea is illustrated in Fig. 2. The forces influencing the suspension MV-97 are shown in Fig. 3. The duckfoot share is in the vertical direction affected by the force G that expresses the gravity of suspension and by the force F_Z, which expresses the gravity of soil and the force needed for turning the soil. Figs. 2 and 3 show the point B, where the dynamometer is fixed and where the force F_{zB} appears. F_{zB} consists of two forces G and F_Z.

The conditions of equilibrium, which are included in equations (5–7), have to be valid because of equilibrium of forces affecting the suspension MV-97 in individual planes. The conditions are determined for work with the equipment to a certain depth and to a certain character of soil. These conditions are valid for the phase of still-stand, for a concave duckfoot share and for the work at given depth of recess into soil of certain characteristics.

1. The equation (5) has to be valid for equilibrium of forces in the horizontal plane.

$$\sum F_x = 0 \qquad \text{(N)} \qquad (5)$$

$$F_{x2} - F_{x1} = 0$$

$$F_{x2} = F_{x1}$$

where: F_{x1} – force recorded by dynamometer No. 1 (N),
F_{x2} – force for soil separating (N).

2. The equation (6) is valid for equilibrium of forces in the direction of axes z.

$$\sum F_z = 0 \qquad \text{(N)} \qquad (6)$$

$$+ F_{zA} - G - F_z + F_{zB} = 0$$

where: F_{zA} – the force influencing suspensions' bearings (N),
F_{zB} – the force recorded by dynamometer No. 2 (N),
F_z – the force expressing soil gravity and the force needed for turning the soil (N),
G – the suspensions' gravity (N).

3. For equilibrium of moments to the point A is valid following condition – equation (7).
   a) The conditions of equipment calibration, the duckfoot share is not affected by the force F_Z on condition of still-stand and given concavity.

$$\sum M_A = 0 \qquad \text{(N.m)} \qquad (7)$$

$$G \,.\, d - F_{zB} \,.\, e = 0$$

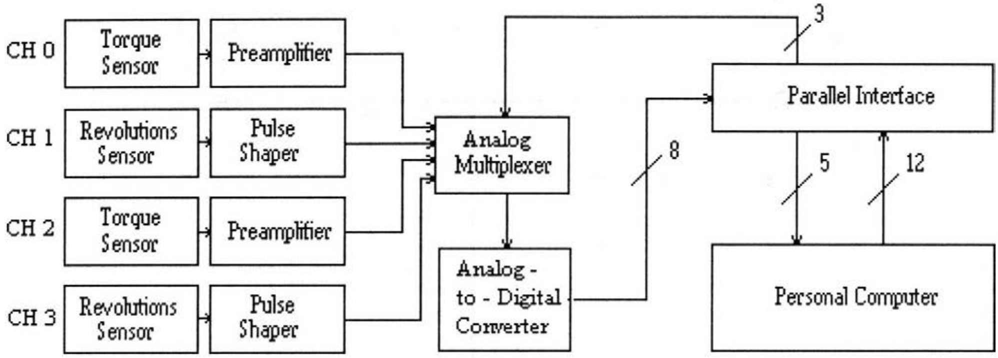

Fig. 4. System of amplifiers

$G \,.\, d = F_{zB} \,.\, e$

where: G – the gravity of suspension (N),
F_{zB} – force recorded by dynamometer No. 2 (N),
d, e – ever arms, that are affected by forces (m).

When measuring, we need to eliminate force B, which expresses the pressure of suspension. That could be reached by trimming before the act of measuring. The measuring software program enables the elimination of moment caused by the force G and F_{zB} that influences the lever arm e.

b) The conditions of measuring – the measuring equipment records the force F_{X1} and the duckfoot share is influenced by the force F_Z. The equation (7) could be expressed in a simpler form as shows equation (7).

$$\sum M_A = 0 \qquad \text{(N.m)} \qquad (8)$$

$$+F_z \,.\, d - F_{zB} \,.\, e - F_{x2} \,.\, a = 0$$

$$F_z = \frac{+F_{x2} \,.\, a + F_{zB} \,.\, e}{d}$$

If we establish $F_{X2} = F_{X1}$ from the equation (5), we will obtain the equation (8).

$$F_z = \frac{+F_{x1} \,.\, a + F_{zB} \,.\, e}{d}$$

The parameters are equal to those mentioned in equation (7). The value of F_{X1} is recorded by dynamometer No. 1 and the force F_{zB} by dynamometer No. 2. The exact value of force F_z, which appears in the vertical plane of the working element, is expressed in the equation (8).

b) Electronic element of measuring equipment MV-97

We designed and constructed a measuring system regulated by computer. The aim of this system was to record and to measure the magnitude of forces affecting agricultural machines in all conditions. The system was

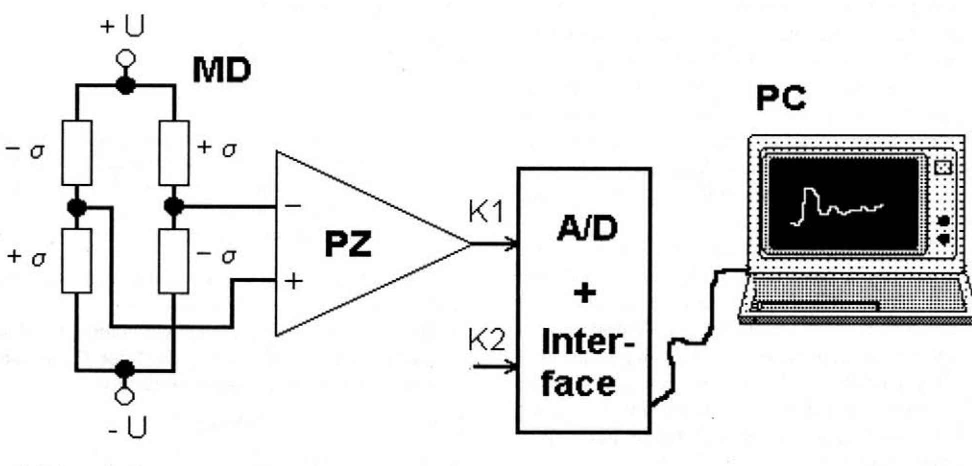

Fig. 5. Schematic diagram of amplifiers' connexion

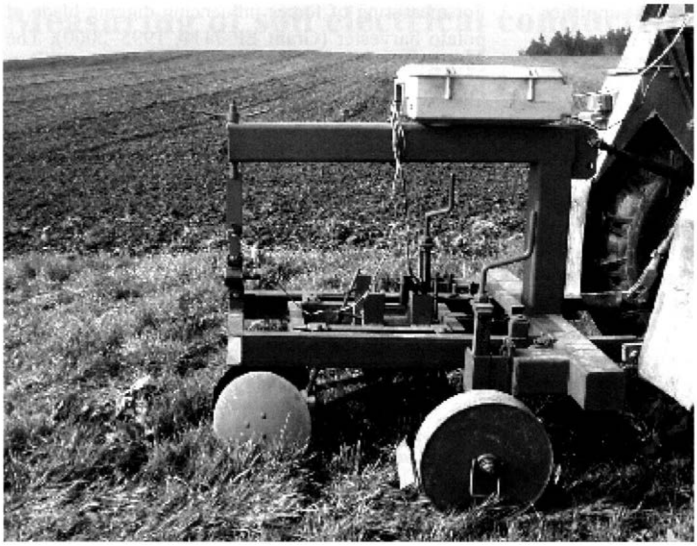

Fig. 6. Complex view on measuring equipment MV-97

experienced by similar proposals /xx/, /yy/, /zz/ (ADÁMEK 1994, 1999; FRÍD et al. 1998, 1999a,b).

This mobile system consists of one power supply +12 V, that includes an analog-to-digital converter, two transistor amplifiers for the recording of signals from tension dynamometers, and a special interface to connect the computer via a standard parallel interface. The system also includes an inductionless converter of voltage –12 V for analog circuits. We designed software for obtaining data and testing the system. This equipment provides already measured values in a form of a measuring protocol – including all necessary data about the research and conditions of the research. The view on the protocol is expressed in text files (see the block scheme of measuring equipment in Fig. 4).

Signals recorded by tension dynamometers with semiconductor sensors FABX – 50 – 12 S6 that are in bridge connexion should be at first 10^3 times amplified and then reverted to analog – digital (A/D) converter and afterwards to the PC interface (see Fig. 5). We put a great burden on the amplifier – in terms of linearity and low temperature drift. These requests are important in order to come closer to temperature stability given by digitalization of signal and for greater precision. We chose the connexion with operational amplifiers – so called transistor amplifiers. Our decision was based upon the

Fig. 7. Measuring of digging blade's resistivity while potato digging

knowledge that within 0 to 85 degrees this amplifier reaches a linearity and temperature drift with measuring error lower than 0.5%.

According to current claims on recording and presentation of measured data on computer we decided to use the interface with standard parallel interface (Printer Port). The Printer Port is the most common and the most universal interface that every computer is equipped with – even notebooks. Thanks to the interface circuit built in to computers we were also able to measure the required parameters on machines moving in fields. This equipment is based on the idea of logic expander of data transferors in the parallel port to printer and it is changed from output device to bi-directional device. The device records all data from A/D converter (12 bit) and the conductors are used as location and controlling.

c) Software for measuring and evaluation of data

The program is controlled on computer from the menu by cursors and the Enter and Esc keys. The name of the program in menu is Tah 1530k.

The data can be reprocessed and presented in the form of graphs. We could use standard software programs such as spreadsheets and word processors and other Windows applications.

d) Utilization of measuring equipment

Our solution enabled continuous measuring and recording of forces influencing the duckfoot share in real time. The taken measurements proved the versatility of the equipment. The measuring system MV-97 was used from 1996:

1. For measuring of forces affecting duckfoot shares.
2. For measuring of forces affecting the ploughshare and ridging plough of potato planter (Grant EP 7111, 1995–2000). The connection of the working elements is shown in Fig. 6.
3. For measuring of forces influencing digging blade of potato harvester (Grant EP 7111, 1995–2000). The connection of the working elements is shown in Fig. 7.
4. For the measurement of tyres' roll resistance.

References

ADÁMEK P., 1999. Vybavení školních laboratoří měřicí a výpočetní technikou. In: Modernizace výuky v technicky orientovaných oborech a předmětech. Olomouc, Univerzita Palackého: 293–295.

ADÁMEK P., 1994. The High-speed Measuring System for the Probe Diagnostics ot the Plasma. In: Proc. of Contribution Papers, Physica of Plasmas and Ionized Media. Faculty of Mathematics and Physics, Charles University, Prague: 60–65.

ANKEN T., HEUSSER J., SARTORI L., 1993. Stoppelbearbeitung, FAT-Berichte. Schweiz. Landtechnik, *55*: 23–32.

BRZKOVSKÝ K., 1965. Zemědělské stroje. [Skriptum.] Praha, ČVUT: 95–137.

FRÍD M., FROLÍK J., ADÁMEK P., 1998. Stanovení parametrů pohonných jednotek pásových dopravníků. In: Ekologické aspekty výzkumu, vývoje a provozu zahradnické techniky. Brno, MZLU, ZF: 59–62.

FRÍD M., ŠABATKA J., ADÁMEK P., 1999a. Měření orebního odporu pracovních orgánů pro zpracování půdy. In: Zemědělská technika na přelomu 20. a 21. století. Praha, ČZU: 22–26.

FRÍD M., FROLÍK J., ADÁMEK P., BLAŽEK V., 1999b. Systém pro měření energetické náročnosti strojů. In: Zemědělská technika na přelomu 20. a 21. století. Praha, ČZU: 27–30.

HŮLA J., MAYER P., 1995. Faktory působící na měrný odpor pracovních orgánů radličkových kypřičů. Zeměd. Techn., *41*: 151–156.

JÄGER P., FUNK M., 1994. Gezogene Geräte arbeiten kostengünstig. DLZ, *45*: 72–81.

Received 21 March 2002

Zařízení pro měření sil působících na šípové radličky

ABSTRAKT: V souvislosti s řešením výzkumného záměru CEZ: J06/98 122200002/I bylo navrženo, zkonstruováno a odzkoušeno měřicí zařízení MV-97. Zařízení umožňuje snímání sil, které působí na symetrické pracovní nástroje pro zpracování půdy ve vertikální a horizontální rovině. Návrh konstrukčního řešení mechanické části aparatury vychází z teoretického rozboru sil, které působí na jednokloubový závěs, a podmínek pro rovnováhu sil u závěsu s opěrným kolečkem. Elektronická část zařízení se software a personálním počítačem tvoří samostatnou část měřicí aparatury, umožňující snímání a průběžný záznam naměřených hodnot do paměti PC.

Klíčová slova: šípové radličky; snímání sil; jednokloubový závěs; dynamometry; personální počítač

Corresponding author:

Ing. MILAN FRÍD, CSc., Jihočeská univerzita v Českých Budějovicích, Zemědělská fakulta, Studentská 13, 370 05 České Budějovice, Česká republika

tel.: + 420 387 772 635, fax: + 420 387 772 630, e-mail frid@zf.jcu.cz

Measuring of soil electrical conductivity for mapping of spacial variability of soil properties within a field

O. ŠAŘEC, P. ŠAŘEC, V. PROŠEK

Czech University of Agriculture, Prague, Czech Republic

ABSTRACT: The purpose of this paper is to discuss the potential usefulness of electrical conductivity maps when interpreting spatial variability in soil properties within a field. The two primary methods of measuring electrical conductivity of soil consist in using either a non-contact sensor based on electromagnetic induction or a coulter-based sensor enabling a direct contact. Soil electrical conductivity measurements have long been used to identify soil differences in the field of geological and archaeological researching. New opportunities for electrical conductivity maps consist in assisting the decision-making process put up within landscape recultivation as well as within precision farming. Concerning precision farming applications, soil electrical conductivity maps provide the highest value when used by GIS software in conjunction with other information as are yield maps, fertility sampling data, soil survey, local agronomic knowledge etc. This helps to reduce input costs such as those of seeds, fertilizers, chemical protection, helps to increase yields, and provides benefits to the environment as well. Another scope that this method may be employed in is soil bank reclamation where it can help to identify points of strong soil differences that have to be modified.

Keywords: electrical conductivity; electromagnetic induction; maps; reclamation; precision farming; GPS; GIS

Those who want to start up with precision management should know well the land that they take care of. Currently, yield maps are the most widespread tool. Generally, they quantitatively show the way in which seed yields changed throughout a field in various years. But these maps do not say indeed anything about the reasons behind the spatial yield variations, i.e about soil properties such as soil type, clay content, organic matter content, water holding capacity/drainage, nutrient provision, topsoil depth and surface profile, which all influence the yield. As well, they do not help us to answer such questions as whether to apply more fertilizers in areas that exhibit higher yields because more nutritive matter was drawn from there, or in contrary whether to apply more fertilizers in areas of low yields because of an assumed nutrient shortage there.

If we wanted to map soil properties of a field using classical methods, it would have involved a large number of samples and their subsequent laboratory analysis. It is very laborious, demanding, and lengthy. These drawbacks can be moderated by the use of sensors that measure electrical conductivity of soil. Data obtained by the sensors and their integration with the data from a differential GPS (Global Positioning System) enable to create maps that show soil differences throughout a field.

MATERIALS AND METHODS

SOIL ELECTRIC CONDUCTIVITY MEASUREMENT

Electrical conductivity represents a material's ability to conduct electrical current. The magnitude of this ability differs according to the material, e.g. sands have a low conductivity as compared to clays. There are two basic methods of measuring soil electrical conductivity. One is a non-contact method based on electromagnetic induction, the other a direct-contact method using coulters. Both non-contact as well as coulter-based sensors make use of either a direct or an alternate electrical current on a low frequency. These methods are not new – for example geologists and archaeologists use probes operating on similar principles when searching for tectonic dislocations, mineral seams, or metal objects. But it is not until now that a wider application of these methods within precision farming puts up thanks to the connection with the GPS that enables to process measured data into maps.

Sensors used may be actuated by hand, self-propelled, or heaved at. Hand actuated sensors are used mainly to measure chosen localities within field investigation and research. Self-propelled and heaved sensors can collect data in question continually during their movement (on-the-go), and make therefore feasible to map the entire lot.

Coulter-based sensors measure soil electrical conductivity by means of coulter electrodes, which stay in direct contact with soil. For example a six-electrode sensor uses the middling pair of electrodes to transmit an electrical current into soil, and hence to create approximately elliptic electrical arrays (Fig. 1). The central and the outward pair of coulter electrodes measures the voltage drop. For the electrical current, the soil represents a resistance that can be calculated via at once the measured voltage drop between the electrodes and the known magnitude of electrical current. The conductivity

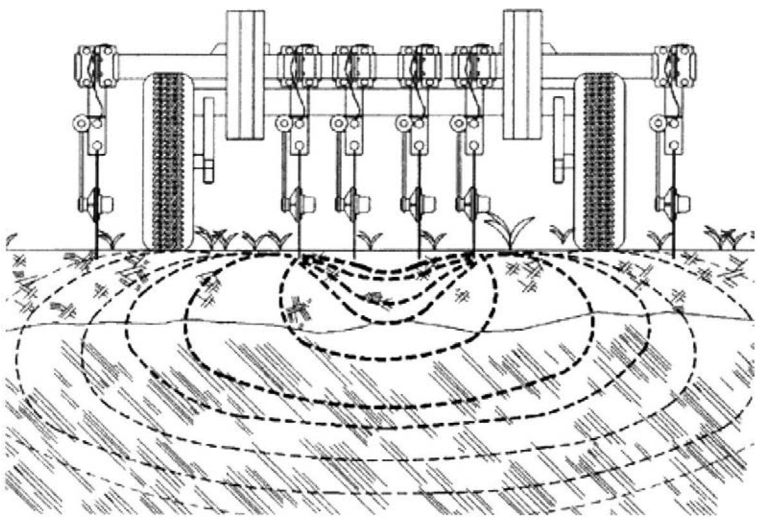

Fig. 1. Six-electrodes instrument for measuring of soil electrical conductivity

is the inverse value of the resistance. MilliSiemens per meter (mS/m) is the standard unit of measure of bulk soil conductivity. The distance between the electrodes of one pair determines the inspected soil depth, while the number of pairs of electrodes determines the number of inspected layers. The six-electrode instrument can measure conductivity over two layers, an approximately 0–30 cm depth as well as a 0–90 cm depth. The rule is that with the increasing distance between the electrodes, the electrical current field reaches deeper. In particular, soil electrical conductivity depends upon soil moisture, salinity, clay and sand content, degree of soil compression, and organic matter content. Soil temperature is another factor that influences soil conductivity. Inaccuracies significantly increase at below-zero temperatures. Straw and other post-harvest residues may as well have disruptive effects on the measurement accuracy.

Non-contact sensors do not have a direct connection to the soil. They consist of a unit generating inductive electromagnetic field, which is then transmitted into the soil, and of a receiver unit measuring response. Researches confirm that both methods provide more or less similar results.

The system records the conductivity measurements together with the position data obtained by the GPS, stores the resulting data in a digital form, and process them into maps. The most important are the measurements that are carried out over the layer of plants' root system, where nutrients are drawn from. When using the sensors, it is possible to promptly create electrical conductivity maps which predicate spatial variances in soil properties of the field in question. In order to correctly specify the causes of the variances, it is necessary to take samples, and then to analyse them in a laboratory. However, the sensors offer a substantial advantage through the reduction of the number of required samples, i.e. we can focus on the arrays with distinct soil variances and subsequently precisely map the entire lot.

RELATIONSHIP BETWEEN SOIL ELECTRICAL CONDUCTIVITY AND SOME SOIL PROPERTIES

For plants, soil is the factor of major importance, and therefore it is not surprising that the maps of soil physical characteristics and the yield maps strongly correlate to each other. Electrical conductivity may serve to express some soil physical characteristics such as organic matter content (JAYNES et al. 1994), clay content (WILLIAMS, HOEY 1987), and cation exchange capacity. The above mentioned characteristics have a considerable impact on the soil's ability to hold water and nutrients, which are the major factors affecting yield. The relationship between soil electrical conductivity and yield was marked as well by other researchers. By means of soil electrical conductivity, it is possible to monitor and to allocate soil salinity (RHOADES, CORWIN 1981), to measure and to discover many other soil's chemical and physical characteristics including moisture (KACHANOSKI et al. 1988), exchangeable Ca and Mg, width of claypan horizon (DOOLITTLE et al. 1994), organic-originating nitrogen. Finally, it is possible to variably adjust applied amounts of herbicides (JAYNES et al. 1994).

RESULTS AND DISCUSSION

In a short-time period, the spatial patterns and areas with different soil characteristics identified by soil electrical conductivity scanning do not change (only characteristics' magnitudes change), and are therefore consistent and repeatable even though these measurements are carried out under different moisture, temperature, and soil compactness conditions (i.e. after sowing, after harvest).

Within precision farming, when evaluating mutual relations between two sets of data, the regression analysis of those data couples is often used. If soil electrical conductivity and yield data sets are analysed, a statistically significant correlation of about 0.6–0.7 (at significant level $\alpha = 0.01$) between them is a customary outcome. The correlation coefficient size can be explained by the dependence of both data sets upon soil properties by whose these data sets are strongly influenced. An interval on which data are collected is another factor of irregularity when taking into account that an electrical conductivity sensor and a yield sensor do not necessarily record exactly the same place in the field (this difference may be caused by an inaccuracy of the GPS etc.). The correlation coefficient is the first important step towards the detection of reasons behind the yield's spatial variances. The visible resemblance of the maps and the data correlation indicate that the mutual relations between the data sets are not accidental. Anyway, the correlation between soil electrical conductivity and yield is too complex to be explained through a mere linear regression. To give an example, this relationship is rarely linear. This is why a model was designed in which yield reaches the highest magnitude somewhere in the middle of the electrical conductivity interval thanks to an optimum balance between soil electrical conductivity and soil hydraulic conductivity there. Yet another fact must be taken into account. The relation between electrical conductivity and yield may change from year to year because of precipitations. This phenomenon must be reckoned with when yield data from several years are to be normalized and averaged. There are many other methods of analysing the relationship between yield and electrical conductivity, e.g. the "border line analysis" may be employed. This method isolates the highest yields within each given electrical conductivity bend, and expresses the highest yields of each band using a non-linear equation.

EMPLOYING SOIL ELECTRICAL CONDUCTIVITY AND YIELD DATA IN FIELD PRODUCTIVITY MANAGEMENT

Many farmers are afraid of applying information on yields (even from several years) when determining production potential areas of a lot, because formerly attained yields are not adequate enough to demarcate those areas. Since insufficient amounts of some inputs (for example nitrogen) manifest in terms of economy, there is a reluctance to cut back these inputs in areas showing lower yields, where there is an inferior overall production potential. Confirmed monitoring has proved that in order

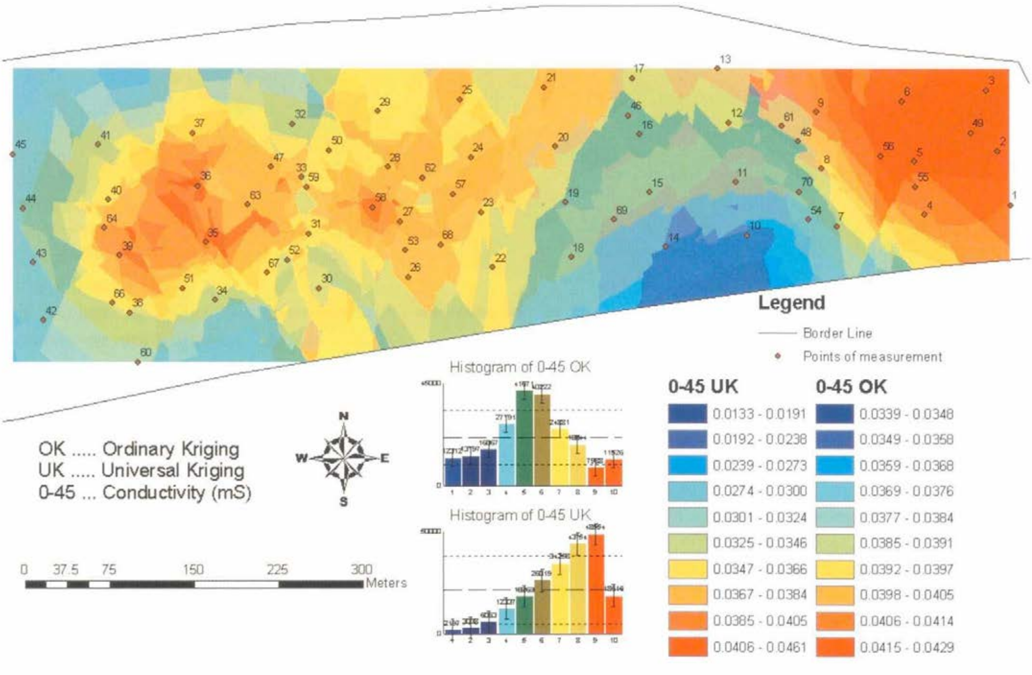

Fig. 2. Conductivity of soil in soil profile 0–45 cm (April 25, 2001)

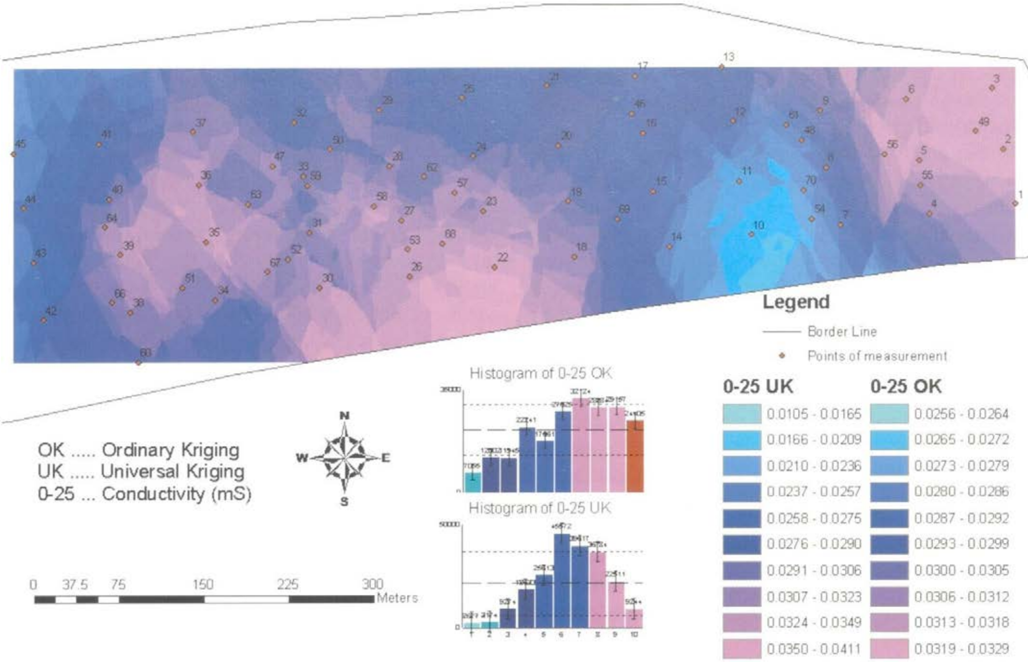

Fig. 3. Conductivity of soil in soil profile 0–25 cm (April 25, 2001)

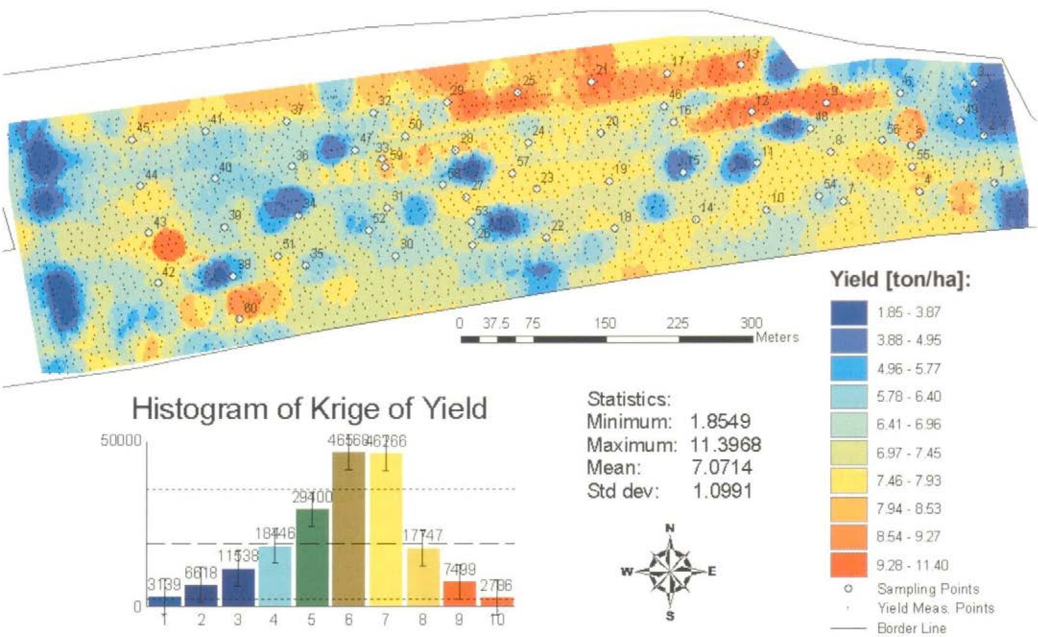

Fig. 4. Yield of winter wheat in 2001

to demarcate production areas of a lot with the use of yield data only, it is necessary to have available information of at least 7–10 years. Another investigation shows that these areas change after an about six-year period. A research on variable rate nitrogen fertilization pointed out improved economic results when spatial information on physical characteristics and yields were incorporated into management. The relationship between soil electrical conductivity and yield can be used for mapping of higher production potential areas. Afterwards, this knowledge may be put to use when applying variable nitrogen rates. In that case, economic outcomes are far better compared with the application of an even amount of nitrogen within the whole lot. Naturally, before the application of any substance according to an individual recipe created with the help of a yield potential map, it is essential to determine the mutual relations between a soil type and a substance that is to be applied. For example a lower yield in areas, where a higher electrical conductivity has been measured, may be caused by either denitrification, or by a shallow topsoil depth. In the latter case, the yield could be really amplified through a higher amount of nitrogen input.

EXAMPLES OF SOIL ELECTRICAL CONDUCTIVITY AND YIELD MAPS

In order to illustrate the problem, field trials were carried out by the Department of Machinery Utilization when the winter wheat was coming out of dormancy in spring 2001. The electrical conductivity data were scanned by a hand-actuated six-electrode instrument (the direct method) with the use of the GPS. The data were processed into two maps, each showing electrical conductivity over a different depth (Figs. 2 and 3). As well a yield map (Fig. 4) is included that enables to compare visually its spatial pattern to the patterns of the two electrical conductivity maps.

CONCLUSION

Within an adequate field scanning, soil conductivity may partially substitute the method that involves a take-off of soil samples and their subsequent laboratory analysis. In other words, the correlation between soil electrical conductivity and yield is larger, if the yield depends primarily on water holding capacity. Fortunately, the spatial variances in soil conductivity of an individual lot tend to remain approximately the same from year to year, unless they are influenced by e.g. a downhill soil erosion.

The easiest way of interpreting soil conductivity map is its visual comparison with the corresponding yield map, or soil scanned map. The boundaries expressed in these maps clearly put forward the resemblance of the areas that exhibit soil properties differences, and of the areas that reach different yields. Electrical conductivity may be as well compared with other measured properties such as degree of declination of a field, plant density, and with the maps of plants height, colour and density gained via an aerial scanning.

Within landscape reclamation, e.g. after coal mining, an investigation of soil variances can make use of electrical conductivity maps. Soil of an area that has undergone a reclamation is distinctly heterogeneous, which poses problems in the process of replanting. Soil conductivity mapping discloses this heterogeneity, subsequent soil sample analysis helps to find out the causes, and finally, necessary and focused measures can be adopted in order to eliminate the extreme heterogeneity. These measures may reduce the replanting costs of the reclamation areas.

The way of utilization of soil conductivity maps differs in consonance with grower's needs, region's conditions, or with the ability to exploit obtained data. For farmers, in order to take advantage of measured data more effectively, and to analyse spatially, it is worthwhile to employ the GIS (Geographical Information System) rather than a simple mapping software.

References

DOOLITTLE J.A., SUDDUTH N.R., KITCHEN N.R., INDORANTE S.D., 1994. Estimating depths to claypans using electromagnetic induction methods. J. Soil Wat. Conserv., *49*: 34–42.

JAYNES D.B., NOVAK J.M., MOORMAN T.B., CAMBARDELLA C.A., 1994. Estimating herbicide partition coefficients from electromagnetic induction measurements. J. Environ. Qual., *24*: 32–35.

KACHANOSKI R.D., GREGORICH E.D., VAN WESENBECK I.J., 1988. Estimating spatial variations of soil water content using noncontacting electromagnetic inductive methods. Can. J. Soil Sci., *68*: 134–136.

RHOADES J.D., CORWIN D.L., 1981. Determining soil electrical conductivity-depth relations using an inductive electromagnetic soil conductivity meter. Soil Sci. Soc. Amer. J., *45*: 234–238.

WILLIAMS B.G., HOEY D., 1987. The use of electromagnetic induction to detect the spatial variability of the salt and clay content of soils. Austral. J. Soil Res., *25*: 7–11.

Received 18 December 2001

Měření elektrické vodivosti půdy za účelem mapování jejích vlastností

ABSTRAKT: Účelem příspěvku je pojednat o přínosu map, vytvořených zařízením měřícím půdní vodivost, při interpretaci prostorových rozdílů půdních vlastností na pozemku. Pro měření půdní vodivosti jsou používány dvě základní metody, a to bezkontaktní, která využívá elektromagnetickou indukci, nebo kontaktní, založená na senzorech dovolujících přímý kontakt s půdou. Zařízení pro měření půdní vodivosti jsou již dlouhou dobu využívána v geologickém a archeologickém průzkumu. Perspektivní je použití map elektrické vodivosti půd při rekultivaci krajiny a v systému precizního zemědělství pro podporu rozhodovacích procesů. Při využití těchto map v systému precizního zemědělství jde o porovnání map pomocí GIS programů s dalšími informačními vrstvami, jako jsou výnosové mapy, mapy zásobení půdy živinami, půdní průzkum, historická znalost pozemku atd. To může pomoci snížit náklady vstupů, jako jsou osivo, hnojiva nebo chemická ochrana, a zvýšit výnosy při současném snížení zatížení životního prostředí. Mapování elektrické vodivosti je možné využít při rekultivacích krajiny, a to ke zjištění lokalit s výraznými rozdíly v půdních vlastnostech.

Klíčová slova: elektrická vodivost; elektromagnetická indukce; mapy; rekultivace; precizní zemědělství; GPS; GIS

Corresponding author:

Doc. Ing. ONDŘEJ ŠAŘEC, CSc., Česká zemědělská univerzita, Technická fakulta, 165 21 Praha 6-Suchdol, Česká republika
tel.: + 420 224 383 146, fax: + 420 220 921 361, e-mail: sarec@tf.czu.cz

Lightweight hall for low-cost do-it-yourself house raising

J. LIBRA, J. MAREČEK

Mendel University of Agriculture and Forestry, Brno, Czech Republic

ABSTRACT: The paper presents design of a single-nave hall with the span of 12 m and pole height from 3.0 to 4.5 m. The hall can be used for warehousing goods, garaging vehicles or shedding farm animals. Construction material is mostly round timber. The structure consists of a strut brace frame with reinforced saddle diaphragm beam in longitudinal module 3.6 m, timber binding rafter and transversal trusses. Material, construction type and solution of details meet requirements and possibilities of do-it-yourself manufacture and assembly. The construction system of the hall has options for the rigid damp-proof roof course or for the prestressed canvas made of technical textile with water-proof surface finish. Foundation of the building is on concrete abutments, or – in a less traditional way – on concrete-encased poles in the ground shaft. Optional technical solutions (textile roofing, pole foundations) can reduce the framework costs including roofing by about 9% and total house raising costs by about 45%.

Keywords: agricultural structures; timber framework; textile roofing; do-it-yourself house raising

The present building activities in the branch of agricultural structures are dominated by reconstructions and adaptations. Original construction works originate mostly from the period between the years 1965–1990. In many a case, the structures can be used only with difficulties, however. Although a maximum utilization of the existing construction resources is desirable, the agricultural practice cannot do without new building.

Construction work cost is a very important factor in the situation when many farmers feel any larger building investments as an unbearable economic burden. However, the effort to save money should never lead to inadequately impaired operating and technical parameters of constructions, which is unfortunately often a case.

One of ways how to achieve savings on investment costs without impaired quality is a do-it-yourself house raising and maximum utilization of materials from local sources. This paper presents a technically easy and low cost hall construction design to be used in farming. The most fitted type for the purpose is a single-nave truss hall with the span of 12 (max. 15) m. The lightweight halls of small and medium-scale span without thermal insulation offer a wide range of employment in agriculture for warehousing, garaging and manufacture as well as for a so called aerated-litter shedding of farm animals.

METHODOLOGY

Model facility is a constructional design of shed for fattening pigs on deep litter. Dimensions and one of space arrangement options are presented in Fig. 1. The design is made in extent and details corresponding to the project after construction with the hall span of 12 m,

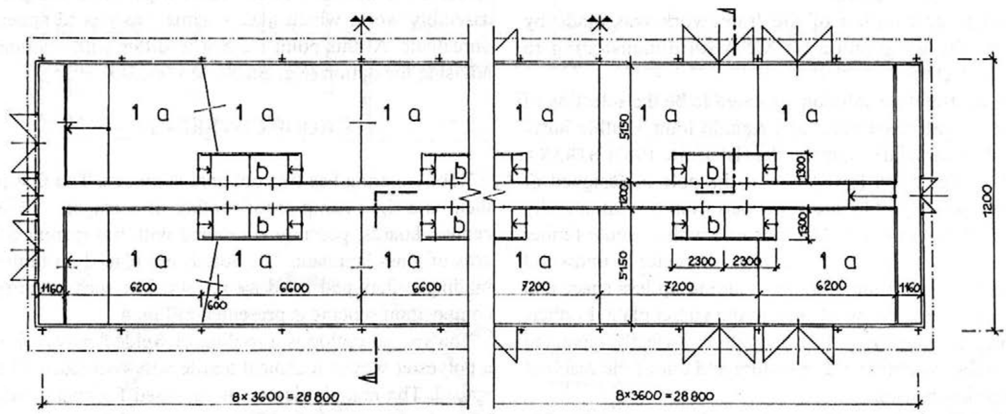

Fig. 1. Pig fattening facility (200 heads) – groundplan
1 – pen for 25 heads; 2 – passage; a – sleeping area; b – feeding place

longitudinal module (truss spacing) of 3.6 m, pole axis height ranging between 3.0–4.5 m. In order to select a suitable solution, the individual supporting and non-supporting frameworks of the model facility were processed in several variants and the solution best corresponding to the chosen conditions was sought by their mutual comparison. In addition to the above mentioned criteria for the selection of material and constructional system the design respects a number of requirements generally imposed on building constructions (adequate strength and rigidity, weather resistance, stall environment hardiness, resistance to mechanical damage, adequate fire safety, unambiguous hygienic character, etc.).

RESULTS – STRUCTURAL DESIGN

ABOVE-GROUND BEARING STRUCTURES

Optimum main building material for do-it-yourself house raising is in this case constructional (soft) timber. Requirements for sawmill and carpentry works are minimal since most constructional elements are in the form of round- or beamwood, i.e. round timber edged on one or both sides. Raw material requirements for the framework are expressed by the share of debarked roundwood diameters in total weight: Ø 150 – 43%, Ø 180 – 15%, Ø 240 – 42%.

The main framework type was selected from a set of possible solutions, which included carpentry constructions, framed nailed structures and joining beams with steel draw-bars (STRAKA, PECHALOVÁ 1991). A system of strut brace frame with reinforced saddle diaphragm beam was classified as most advantageous. Longitudinal reinforcement is ensured with timber binding rafters and transversal trusses located in the plane of roof and end module walls. The location of transversal truss can be accommodated to the requirements of space arrangement. Individual elements of the structure are coupled by means of steel bolts, dowel pins and gusset plates.

Static calculation of the framework was made by using the programme NEXIS with dimensioning to EUROCODE 5.

A contributing solution appeared to be the selection of system with fixed poles and summit joint – rather untypical of carpentry frameworks (HUJŇÁK 1986; STRAKA 1999). The fixed lower part of the pole is designed of steel rolled I profile, the upper part from two unilaterally scarfed timber stiles. As compared with a whole-timber pole, there is a saving in large-diameter roundwood (320 mm), with the strut brace taking up less space and the pole being not weakened in the gusset plate. Furthermore, the wooden part of the pole is perfectly separated from the swelling earth moisture and out of the reach of splashing rainwater.

Weight of the bearing construction including gable poles is 32.8 kg/m^2 groundplan area. The proportion of constructional steel is about 4.6 kg/m^2, i.e. ca 14%.

GROUNDWORKS

Groundworks are considered in two options. The first of them is a common foundation shoe made of plain concrete with bell anchoring of the pole. Shoe size for the Class F5 foundation earth is 1.6/1.0/1.0 m. As the foundation shoe size is in this case conclusively affected by load excentricity, the shoe dimensions are nearly identical even at the pole axis height of 4.5 m.

The second option represents a system of so called pole foundations. The poles are embedded directly into a pre-drilled ground shaft where they are levelled and carefully encased in concrete. Dimensions of the pole foundation depend first of all on the type and consistence of foundation earth and on the depth of structure foundation. The earth of Class F5 for example requires the depth of foundation block 1.8 m and diameter 0.8 m, while the earth of Class S1 would call for the depth of 1.5 m and diameter 0.6 m. The static calculation was made with using a methodology based on DIN 18900 (NÜRNBERGER 1988) and geotechnical values to ČSN 73 1001 (Základová půda pod plošnými základy).

At the "pole" system of foundation it is necessary to extend the steel portion of the pole or we can use a whole-timber pole consisting of one piece of roundtimber which in our case must have a diameter of 320 mm. The whole-timberpole must be depth-impregnated; a similar system is rather widespread in the U.S.A. (Pole building). It can bring certain savings provided that the conditions of foundation are favourable and necessary technical equipment available. In addition to the above described framework modifications it also requires a specific assembling procedure.

A comparison of complete costs for above-ground and foundation structures demonstrated clear benefits of the structure with extended steel part of the pole. The solution is not known from available literature but there are no reasons to cast doubts on its functionality.

However, in the conditions of do-it-yourself house raising the pole foundations represent increased requirements for mechanization (earth auger) and complex assembly work, which makes actual savings to appear unrealistic. At this point we beg to differ with opinions advising the option (e.g. BROŽ, MATOUŠEK 1995).

ROOF COVERING

Roof covering has two optional solutions. The first of them is a rigid damp-proof roofing of corrugated fibre-cement boards, possibly combined with transparent boards of glass laminate. The boards are placed on timber binding rafters and fixed by screws. The roof covering composition scheme is presented in Fig. 4.

The second option is a roofing of welded canvas. It is a polyester woven technical textile with two-sided PVC spread. The material is commonly used for encasement of enclosed arched steel structures, sheds and car-canvases. In foreign countries it also finds use as a free-standing tent construction supported and stretched by a system of masts, cables etc. (ORTON 1991). Its wider use for suspended prestressed constructions is prevented particularly by the necessity of forming the canvas into an unfoldable surface curved in all directions. The manufacture of this canvas cut is technically demanding and more than twice costly.

A benefit of the presented solution consists in the simplicity and flexibility of active canvas stretching system with minimum requirements for tolerances of the supporting construction. The canvas is of simple rectangular shape, its edges being longitudinally reinforced with welded strips. It dwells on round strut beams and stretched in the middle of each module by means of a steel tube inserted into the covering transversal pocket. The proper prestressing occurs by means of steel threaded bars and timber rafter suspended beneath the binding rafters. The resulting fish-net, ultra lightweight and partially transparent roofing can find a range of aesthetic applications. The covering canvas must be factory-made and yet it is by about 60.00 CZK/m^2 (27%) cheaper than the rigid damp-proof course. The guaranteed service life of the two materials is about the same. A certain disadvantage of the canvas consists in its additional stretching after several years.

The simple membrane roofing can be for both variants easily complemented with a reinforced polyethylene foil soffit lightly stretched between the strut beams. The treatment will both increase the structure's heat resistance and facilitate the flowing of overheated air from the inter-roof space outside the object at the summer insolation of the roof. The soffit can be provided with a thermal insulation.

VERTICAL CLADDING

Supporting members of the cladding are horizontal nogging pieces of roundwood anchored to frame and gable poles. The proper cladding then can be as required consisting of shuttering, fibre-cement or glass-laminate boards, technical textiles, grid, or a combination of these materials. Operations with an increased risk of mechanical damage can have a reinforced brick lining carried out up to the level of timber pole part.

A model shed has a filling of batten panels in the lower part of the longitudinal wall, which fulfils the function of wind protection and sty partition. In the upper part there is a stretched external screen of technical textile and an internal net fixed on skew strut braces. The vertical cladding surface can be easily reduced.

It is once again a beneficial atypical solution that makes it possible to markedly suppress the share of "inorganized" infiltration in natural ventilation during the winter period. The internal net provides for channeling the incoming air flow and can also slow down its rate.

APPLICATION

The above construction system can be used for a wide range of warehousing, garaging and farm animal rearing facilities. Its concept particularly meets the requirements of private farmers and smaller agricultural companies. It creates conditions for animal rearing which respects ethological requirements of animals and their welfare.

The option with rigid damp-proof course and flat foundation was applied in a project of stalls, hayloft

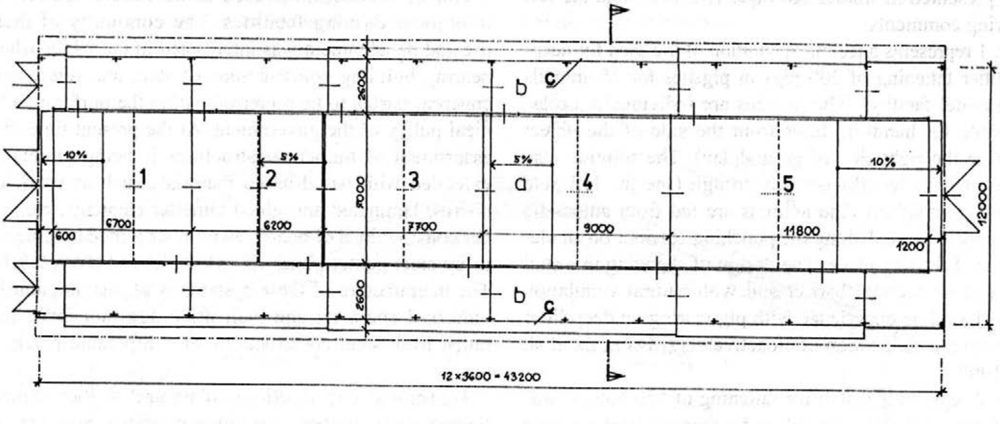

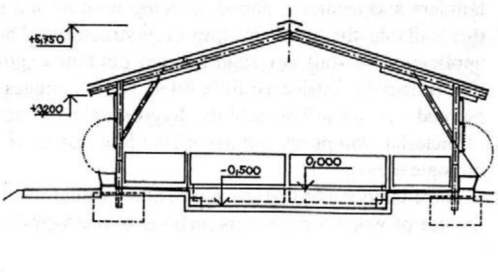

Fig. 2. Bull fattening facility (150 heads) – groundplan; cross section

1 – pen for 2 × 15 heads (4–6 months); 2 – ditto (7–9 months); 3 – ditto (10–12 months); 4 – ditto (13–15 months); 5 – ditto (16–18 months); a – sleeping area; b – feeding area; c – trough

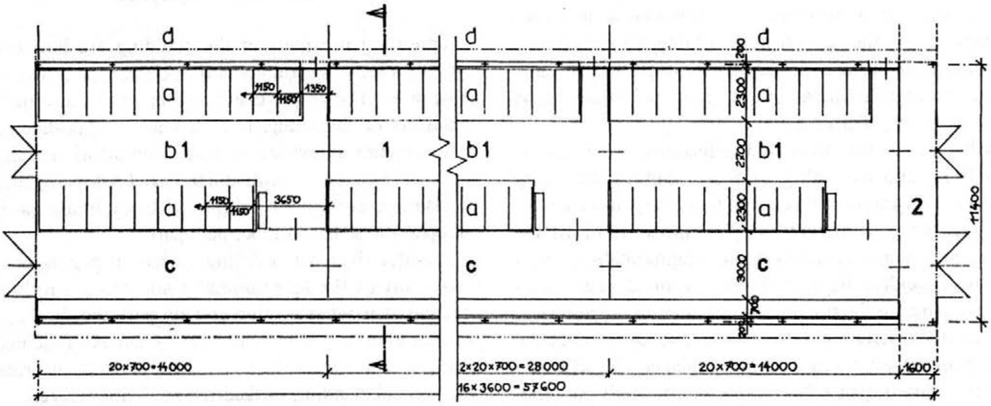

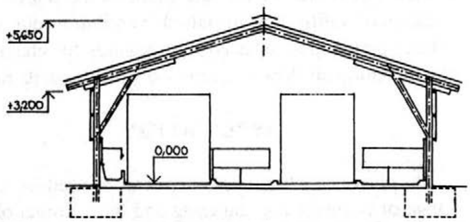

Fig. 3. Dairy cow facility (80 heads) – groundplan; cross section

1 – pen for 20 heads; 2 – passage; a – littered cubicles; b – dung passage; c – feeding area; d – open yard

and barn, which form a manufacturing part of the family beef cattle farm without market production of milk. (Stall cross-section see Fig. 4.) Construction works were launched in 2001, halls will be raised in 2002.

Examples of hall applications to shed farm animals are presented in studies see Figs. 1, 2 and 3 and the following comments:

Fig. 1 represents a technical solution of the shed for deep-litter fattening of 200 pigs in pigsties for 25 animals (model facility). The pigsties are individually accessible for handling litter from the side of the object (see the right side of groundplan). The solution also enables a lengthwise way trough (see the left side of groundplan). The animals are fed from automatic feeders located along the punching corridor on an elevated feeding place. The design of shedding in a stall with no thermal barrier and with natural ventilation is based on experience with pig rearing on deep-litter with the application of bioactivators (MAREČEK et al. 1999).

Fig. 2 represents a stall for fattening of 150 bulls in differentiated stalls for 30 or 50 animals kept on deep litter with an elevated feeding place and roofed outdoor troughs into which the fodder is placed from an external communication running along the stall building.

Fig. 3 represents a production stall for 80 dairy cows divided into groups by 20 animals. Bedding box maintenance with separate feeding area which at the same time serves for passing of the feeding carriage. The solution saves surface area and its functionality is guaranteed thanks to the consistent separation of a so called quiet zone.

DISCUSSION

Timber constructions used to be widely applied in traditional farming facilities. The continuity of their use and development was interrupted in the 1960s when bearing building constructions of steel and reinforced concrete started to be preferred within the uniform technical policy of the government. At the present time, the assortment of timber constructions is being gradually extended with wood-based materials such as particle-boards, laminated and glued lamellar elements, etc., or bar constructions of board sawntimber joined by glueing or by steel gusset plates (KUKLÍK, KUKLÍKOVÁ 2001). The manufacture of these systems is of unambiguously industrial character and their price does not differ too much from steel constructions of comparable parameters.

Traditional constructions of natural timber (round timber, sawn timber) are perceived by a majority of builders and technical public as being inferior and rather suitable for small or temporary structures. Their application in stall environment and outdoor exposition is usually considered little fitted. Disadvantages to pointed out are inflammability, hygroscopic character of material, dampness and associated low resistance to biological pests.

There is no doubt that these properties would restrain the use of wood for the constructions of multi-storeyed

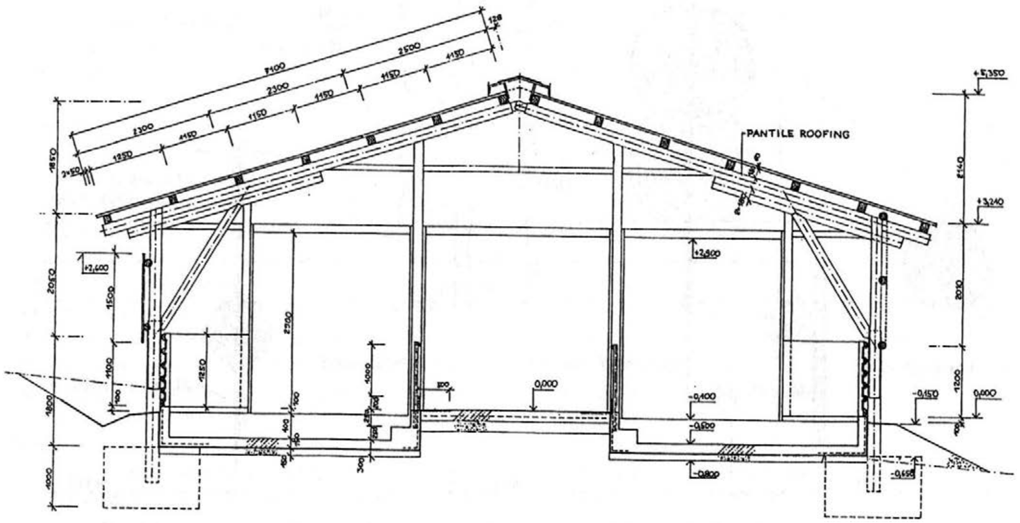

Fig. 4. Cattle fattening facility (35 heads) – cross section

facilities, for the lower structure, for wet operations and the like. Nevertheless, for the above described halls the risks can be eliminated by the structural design and by the secondary protection of timber.

The presented structural design eliminates a possibility of wood material contacting a permanently damp environment and ensures a maximum protection of outdoor part of the structure against weather impacts (roof overlapping, cladding and coverage of members). No part of the construction is hermetically enclosed and its contact points are designed in such a way that they cannot retain rain- or condensed water. Even in the conditions of stall environment with the relative air humidity ranging between 80–85% the construction can be classified in the Danger Class 2 with the exception of a smaller portion of exterior members that are classified in Class 3 (ČSN-EN 335). All this indicates that the secondary (chemical) protection is not too demanding. It should consists of a mere surface impregnation against biotic pests, which is combined in the exterior with a surface treatment against weather impacts (ŠIMŮNKOVÁ 1998). As compared with a similar steel construction, the maintenance requirements are lesser in interior and identical in exterior.

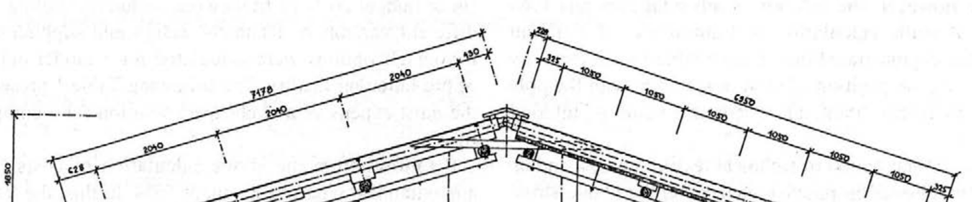

Fig. 5. Pig fattening facility – cross section

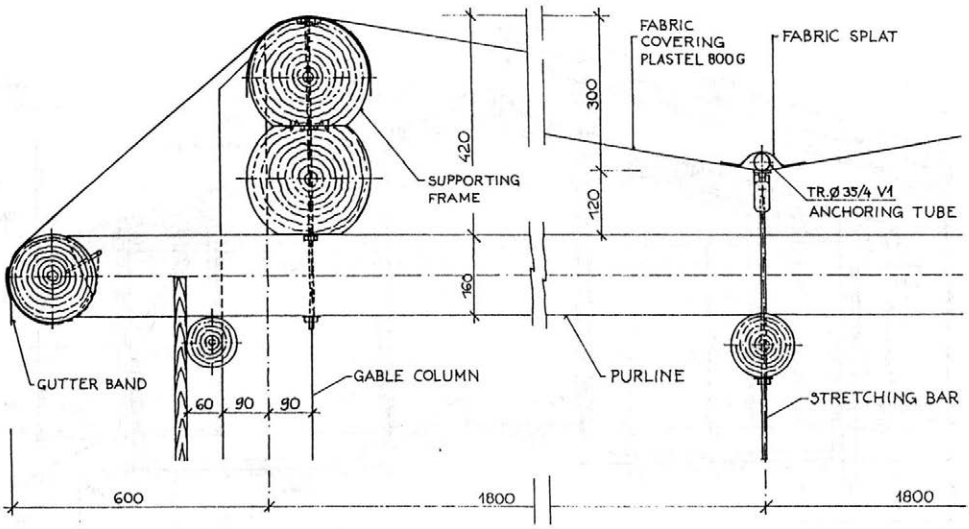

Fig. 6. Roof canvas anchoring and stretching – details

Inflammability of the construction material is acceptable for the designed object type. Its fire resistance can be much better than that of unprotected steel construction, which means that in general the object can be classified in a higher degree of fire safety.

The chosen construction system of single-joint strut brace framework has an entirely adequate weight and requirements for dimensions of roundwood. Its manufacture is relatively little laborious and the framework principle showed most beneficial at the given dimensions. A functional disadvantage is the inclined shore which puts some limitations on the cross-sectional profile of the object. Seen from the static point of view, however, the solution is advantageous and low-cost. A static calculation of frameworks of different heights demonstrated that it is possible to achieve – by changing the position of strut brace node with the pole – a practically identical course and value of internal forces.

The roofing option of technical textile is a new and up to now untested in practice element in the above structural design. A realistic possibility of its verification is coming along for the object of beef cattle stall (Fig. 4) in autumn 2002. It will concern first of all a precision of manufacturing and assembling tolerances of the framework, tolerances of local deformations in laying the canvas, adjustment complexity and other details of effective assembling procedure.

Fitness of the construction cannot be casted doubt upon as in this model the canvas disposes of considerable reserves in terms of both strength and elasticity and the construction enables an easy additional stretching in the case of prestress losses occurring due to the long-term shaping of material.

CONCLUSION

The hall concept with frame construction of roundwood with minimum processing and with about 16–18% weight proportion of steel elements meets both functional and implementation requirements. Basic budget costs of framework including roofing for different variants of technical design and supplier/do-it-yourself options were calculated for a model object of pig fattening facility. The following Table 1 presents the most expensive and cheapest solution for a comparison.

It follows from the above calculation of costs that a maximum saving can be about 55%. In this, the technical options have a share of about 9% with about 46% falling to the do-it-yourself house raising. The solution is quite realistic and does not impose any extreme requirements on the builder provided that the project, technical and organizational preparation of construction works are of good quality. The level of savings depends on the proportion of do-it-yourself work and material (timber)

Table 1. The most expensive and cheapest solution

Structural design option	Investment costs – contractual	Investment costs – do-it-yourself
Spread footing, rigid damp-proof course	825,000 CZK	ca 395,000 CZK
Pole foundations, textile roofing	735,000 CZK	ca 365,000 CZK

from own sources; under an optimum constellation the savings can reach 60%.

Virtue of the presented solution consists primarily in saving costs. However, important is also its social and environmental dimension. The do-it-yourself house raising is a organic component of the tradition in our countryside and plays an important role in forming the village social climate such as at restoring the neighbourhood assistance. The potential of knowledge and skills at semi-professional and professional levels is considerable in the rural communities and when the projects come to materialization, the required mechanization is usually available there. The do-it-yourself house raising realized on a level of the village community can also significantly contribute to alleviation of burdensome unemployment, at least in terms of its psychological impact.

The proposed structural design is environment-friendly thanks to the employment of wood – local and renewable resource. Its processing requires little energy, the material is secondarily utilizable and its character is hygienically unobjectionable.

From the viewpoint of future development, the do-it-yourself house raising, making use of local material and labour sources and based on craftsman skills, is considered by numerous authors (e.g. ABBOT 1993; TRAINER 1995) to be a progressive trend and this technical design fits very well into a broader conception of efforts aimed at the restoration of countryside.

References

ABBOT D., 1993. Organic Traditions. Resurgence, *162*: 26–27.

BROŽ V., MATOUŠEK A., 1995. Dřevěné sloupové konstrukce zemědělských staveb. [Informační list MZe ČR 11/1995.]

HUJŇÁK J., 1986. Dřevěné stavební konstrukce a dílce. Praha, SNTL: 190.

KUKLÍK P., KUKLÍKOVÁ A., 2001. Dřevěné konstrukce na počátku 3. tisíciletí. Stavební listy, 8: 20–33.

MAREČEK J., SYCHRA L., BOČEK B., 1999. Perspektivní systémy využití biotechnologických metod při ekologickém zpracování exkrementů prasat. Nitra, AGROTAR: 42.

NÜRNBERGER W. (ed.), 1988. Informationsdienst Holz. Zweckbauten für die Landwirtschaft. München, Enwicklungsgemeinschaft Holzbau: 31.

ORTON A., 1991. The way we build now: form, scale and technique. London, Chapman and Hall: 527.

STRAKA B., 1999. Využití dřevěné kulatiny v konstrukčních soustavách. Materiály a technologie pro stavbu, 4: 36–38.

STRAKA B., PECHALOVÁ J., 1991. Dřevěné konstrukce. Brno, VUT: 129.

ŠIMŮNKOVÁ E., 1998. Ochrana dřeva proti biologickému napadení a proti ohni. Materiály a technologie pro stavbu, 4: 30–36.

TRAINER T., 1995. Building Highly Self-Sufficient Settlements. In: The Conserver Society. London and New Jersey, Zed Books: 186.

Received 9 May 2002

Lehká hala vhodná pro levnou svépomocnou výstavbu

ABSTRAKT: V příspěvku je uveden návrh jednolodní haly s rozponem 12 m a výškou sloupů od 3 do 4,5 m. Halu je možné využít pro skladování, garážování i ustájení hospodářských zvířat. Konstrukce je převážně z dřevěné kulatiny. Tvoří ji vzpěrkový rám se zesílenou sedlovou příčlí v podélném modulu 3,6 m, dřevěné vaznice a příčná ztužidla. Materiál, typ konstrukce i řešení detailů vyhovuje potřebám a možnostem svépomocné výroby i montáže. Konstrukční systém objektu je řešen ve variantách pro tuhou střešní krytinu nebo předpjatou plachtu z povrstvené technické textilie. Založení budovy je na betonových patkách nebo netradičním způsobem vetknutí sloupů obetonovaných v zemní šachtě. Variantním technickým řešením (textilní krytina, kůlové základy) lze docílit úspory nákladů na nosnou konstrukci včetně střešní krytiny asi 9 %, svépomocným způsobem výstavby 45 %.

Klíčová slova: zemědělské stavby; dřevěná rámová konstrukce; textilní krytina; svépomocná výstavba

Corresponding author:

Ing. JAROMÍR LIBRA, Mendelova zemědělská a lesnická univerzita, Agronomická fakulta, Zemědělská 1, 613 00 Brno, Česká republika

tel.: + 420 545 136 025, fax: + 420 545 132 914, e-mail: libra@mendelu.cz

Effect of adjuvants on spray droplet size of water

M. PROKOP[1], R. KEJKLÍČEK[2]

[1]*State Phytosanitary Administration (SPA), Division of Plant Protection Equipment, Brno, Czech Republic*
[2]*Mendel University of Agriculture and Forestry, Brno, Department of Plant Protection, Czech Republic*

ABSTRACT: Adjuvants (Ekol® – 90% raps fluid, 10% polyetoxyl esters and Agrovital® – 96% pinolene) were evaluated to determine the effect on spray droplet, droplet deposit and another characteristics of droplet spectra. Two kinds of low drift nozzles and one kind of standard flat-fan nozzles LURMARK were used. Water was applied alone and with adjuvants. Agrovital® was mixed at rate of 3 ml/10 l water and Ekol® was mixed at rate of 150 ml/10 l water. Volume Median Diameter (VMD), Number Median Diameter (NMD), boundary volume medians ($D_{0.1}$ and $D_{0.9}$), relative span factor and ratio VMD/NMD was found out for each droplet spectrum. The low-drift nozzles increased VMD and NMD and produced fewer volume of drift prone droplets than standard flat-fan nozzles. Both Agrovital® (Miller Chemical and Fertilizer Corporation US) and Ekol® (JIZA a spol. v.o.s., Czech Republic) increased the droplet size and decreased the percentage of small droplets.

Keywords: Agrovital; Ekol; droplet size; nozzles; spray; spray drift

The use of agrochemicals to control pests in agricultural crops is a widely accepted practice, with most of these products being dispersed into the atmosphere as a liquid spray droplets. The atomization process of converting liquid into spray droplets and fate of the droplets after formation are dependent on physical properties of the formulation, spray volume, nozzle type, nozzle pressure and ambient conditions at the application.

The deposition of fine spray droplets on *Mithimna separata* in flight was 1.49 times more when the spray was produced through an air-mist nozzle than when it was produced through a normal cone nozzle (YAUN-HUIZHU et al. 1997).

A comparison of spinning disc atomizers and flat fan pressure nozzles in terms of pesticide deposition and biological efficiency within cereal crops showed that the Micromax rotary atomizers when operating at a disc speed of 5,000 r.p.m. was found to be the most efficient at all the growth stages examined (HOLLAND et al. 1997).

Fate of droplets, especially the pesticide contained in the droplets, has caused significant environmental concerns related to air and water contamination. The small droplets produced in this process are recognized as a major contributor to off-target drift, resulting in environmental contamination. These environmental concerns have prompted increased interest in the development of improved methods of application that will minimize environmental contamination (HANKS 1995).

SUNDARAM et al. (1992) found out that the addition adjuvants (Sta-Put and Chem-Trol-polyvinyl polymer – 1%) caused increasing of VMD (Volume Median Diameter) and NMD (Number Median Diameter), while the small droplets were reduced.

For practical purposes, the distribution of droplet sizes in a spray may be represented concisely as a function of two parameters, one of which is a representative diameter and the other a measure of the range of sizes. There are many possible choices of representative diameters each of which could play a role in defining the distribution function. The following were used: $D_{0.1}$ = droplet diameter where 10% of the total liquid volume is in droplet of smaller diameter; $D_{0.9}$ = droplet diameter where 90% of the total liquid volume is in droplet of smaller diameter; VMD (Volume Median Diameter) = droplet diameter where 50% of the total liquid volume is in droplet of smaller diameter ($D_{0.5}$). In addition to the volume median diameter (VMD), the number median diameter (NMD) is also used. It is defined as a diameter which divides the total number of droplets into two equal parts, i.e. half the total number of droplets is contained in smaller droplets and half in larger droplets (LEFEBVRE 1993).

Ratio VMD/NMD and relative span factor are used for indicating of breadth of the droplet spectra. Relative span factor is defined as $\Delta = D_{0.9} - D_{0.1}/VMD$. It provides a direct indication of the range of droplet sizes relative to volume median diameter (LEFEBVRE 1993).

One of the criteria used to judge the efficiency of pesticide application is the density of spray droplet deposits per unit of leaf area, usually expressed as droplets/cm². The recommendations for herbicide applications range

This paper is a part of the Project Ministry of Education, Youth and Sports CEZ: J08/98: 4310001.

Table 1. Characteristics of droplet spectra for water only (μm)

Nozzle	VMD	NMD	$D_{0.1}$	$D_{0.9}$	VMD/NMD	Relative span factor
015F110	182.45	62.86	75.97	296.52	2.90	1.21
03F110	267.12	99.11	112.56	380.46	2.70	1.00
05F110	389.44	156.98	198.23	639.30	2.48	1.13
LD015F110	246.96	97.78	106.43	384.52	2.53	1.13
LD03F110	345.29	139.12	151.81	556.03	2.48	1.17
LD05F110	484.21	103.62	206.61	856.07	4.67	1.34
DB015F120	337.75	137.64	156.90	503.76	2.45	1.03
DB03F120	568.48	149.63	267.41	776.76	3.80	0.90
DB05F120	910.79	199.61	464.42	1,255.09	4.56	0.87

from 25 to 30 droplets/cm², for fungicides from 50 to 70 droplets/cm² and for insecticides from 30–40 cm² (BLAHOVEC, ŘEZNÍČEK 1988; TRUNEČKA 1992).

The density of droplet deposit can be influenced by the adjuvants. REED et al. (1990) found out that mixture of herbicides tridiphane + atrazine enhanced application coverage with an addition of soyabean oil adjuvant.

The density of droplet deposit is influenced by the ability of leaves to capture the spray droplets too. The ability of capturing droplets depends on the surface of leaves. The leaves with hairs on the surface can capture more spray liquid then smooth leaves (TRUNEČKA 1996).

MATERIAL AND METHODS

DROPLET SIZE VERIFICATION AND DROPLET DEPOSIT

Three kinds of nozzles LURMARK and three nozzle sizes for each kind of the nozzles were used to determine the droplet size: 1. FanTin – classical flat-fan nozzles (015F110, 03F110, 05F110); 2. Lo-Drift – antidrift nozzles (LD015F110, LD03F110, LD05F110); 3. Drift-BETA – antidrift nozzles (DB015F120, DB03F120, DB05F120). The droplet size and droplet deposit were estimated by the silicon capture method (Methodology SPA 2000) which consists of capturing spray droplets in Petri plates containing a layer of 500-cS (low-viscosity) silicone fluid (Witco S.A.) covering a layer of 300,000 cS (high-viscosity) silicone fluid (Witco S.A.). Spray droplets at the interface of the two silicone fluid layers were photographed and than measured and counted on the computer screen. 2,000 droplets were estimated for each nozzle and fluid.

RESULTS

WATER

The droplet spectrum characteristics of water are shown in Table 1. Droplet size (VMD) ranged from 182.45 μm for the smallest nozzles and the biggest injection pressure (015F110; 0.4 MPa) to 910.79 μm for the largest nozzles and the lowest injection pressure (DB05F120; 0.15 MPa). Number median diameter ranged from 62.86 μm to 199.61 μm. Table 4 shows the number of droplets under 75 μm, which are important for a drift. The biggest number of small droplets was found in spraying of 015F120 nozzles (1,425 droplets = 71.25%) but more important is the droplets volume to 75 μm. Volume of droplets to 75 μm was for DB05F120

Table 2. Characteristics of droplet spectra for water + Agrovital (3 ml/10 l water – μm)

Nozzle	VMD	NMD	$D_{0.1}$	$D_{0.9}$	VMD/NMD	Relative span factor
015F110	192.68	79.78	88.19	305.95	2.42	1.13
03F110	274.94	111.03	134.37	408.41	2.47	1.00
05F110	445.87	197.57	224.95	706.56	2.26	1.08
LD015F110	257.74	120.55	139.31	416.88	2.14	1.08
LD03F110	382.63	130.02	181.27	546.68	2.94	0.96
LD05F110	527.90	140.03	221.40	756.52	3.77	1.01
DB015F120	406.44	183.29	193.60	591.75	2.22	0.98
DB03F120	615.78	179.92	306.47	837.52	3.42	0.86
DB05F120	939.01	178.55	470.19	1,261.70	5.26	0.84

Table 3. Characteristics of droplet spectra for water + Ekol (150ml/10 l water – μm)

Nozzle	VMD	NMD	$D_{0.1}$	$D_{0.9}$	VMD/NMD	Relative span factor
015F110	193.58	80.93	87.92	301.86	2.39	1.11
03F110	282.09	107.52	130.97	412.41	2.62	1.00
05F110	437.13	197.21	224.64	688.65	2.22	1.06
LD015F110	255.14	120.46	137.41	403.41	2.12	1.04
LD03F110	387.15	126.44	180.43	559.18	3.06	0.98
LD05F110	536.42	142.24	222.45	786.13	3.77	1.05
DB015F120	406.9	191.02	197.38	607.98	2.13	1.01
DB03F120	614.25	209.13	304.38	846.78	2.94	0.88
DB05F120	928.61	183.38	475.32	1,243.69	5.06	0.83

only 0.023% whereas for nozzles 015F110 the droplet volume to 75 μm = 5.573%.

AGROVITAL AND EKOL

The droplet spectrum characteristics of Agrovital® (96% pinolene) and Ekol® (90% raps fluid, 10% polyetoxyl esters) are shown in Tables 2 and 3. The addition of Agrovital® (3 ml/10 l water) and Ekol® (150 ml/10 l water) caused, that more droplets in spray were situated between the boundary diameters ($D_{0.1}$ and $D_{0.9}$). Values of relative span factor were smaller then for water only and the ratio VMD/MND were smaller too in most cases (Tables 1–3). The decrease of droplets volume under 75 μm is important (Tables 4–6). The adjuvants were possible increase VMD and reduce the volume of spray in small driftable size particles.

The low-drift nozzles increased VMD and NMD and produced fewer volume of prone droplets than the standard flat-fan nozzles (Tables 1–3). Differences were found between two kind of the low-drift nozzles too. The Drift-BETA nozzles produced larger droplets and fewer volume of spray in small driftable particles than the Lo-Drift nozzles (Tables 4–6).

The addition of adjuvants did not increase only values of VMD and NMD but influenced volume of droplets under 75 μm. Bouth Agrovital® (96% pinolene) and Ekol® (90% raps fluid, 10% polyetoxyl esters) decreased volume of driftable particles and droplet deposit on non-target surfaces. This is important for the restriction of pesticide losses and environmental contamination. Increasing of the VMD and the NMD and decreasing of the relative span factor improve the penetration into bottom parts of the plants and the efficiency.

DISCUSSION

Formulation of agrochemicals, as well as the adjuvants and diluents that are mixed with before application, are constantly changing. Combining all of these ingredients into a spray solution represents varying physical properties such as surface tension, viscosity, and density. BOUSE et al. (1990) reported that other formulation factors are important in determining droplet size, when droplet size decreased with increasing concentrations of the adjuvant X-77, but surface tension, viscosity, and specific gravity varied only slightly. Droplet size is not only affected by the ingredients in the spray solution, but also by the order in which the various components are mixed (BERGER, BERGER 1993). Although the physical properties of solutions change, a given atomizer will respond to the changes and pro-

Table 4. Number and volume of droplets under 75 μm

Nozzle	Water			
	Number of droplets under 75 μm	(%)	Volume of droplets under 75 μm ($mm^2/10^3$)	(%)
015F110	1,425	71.25	64,444.75	5.57
03F110	936	46.80	43,832.54	1.10
05F110	456	22.80	35,149.08	0.23
LD015F110	895	44.75	40,918.62	1.14
LD03F110	576	28.80	42,511.10	0.44
LD05F110	1,125	56.25	51,594.46	0.50
DB015F120	604	30.20	25,354.88	0.26
DB03F120	796	39.80	43,738.44	0.19
DB05F120	910	45.50	19,097.47	0.02

Table 5. Number and volume of droplets under 75 μm – Agrovital

Nozzle	Number of droplets under 75 μm	(%)	Volume of droplets under 75 μm (mm^2/10^3)	(%)
015F110	1,136	56.80	54,575.89	2.84
03F110	877	43.85	57,185.01	1.08
05F110	521	26.05	28,786.33	0.11
LD015F110	796	40.05	42,952.94	0.71
LD03F110	847	42.35	34,920.00	0.32
LD05F110	667	33.35	35,250.34	0.21
DB015F120	534	26.70	15,184.29	0.08
DB03F120	812	40.60	27,214.30	0.07
DB05F120	1,001	50.05	21,735.24	0.03

duce droplet size in relation to this change. Droplet size can be significantly affected by tank mixing various pesticides with adjuvants (BOUSE et al. 1990). These solutions are typically applied through a spray system with regard to changes occurring as the solution exit the system as spray droplets.

HANKS (1995) compared the droplet spectra of water only and with adjuvants (Sta-Put and Chem-Trol-polyvinyl polymer – 1%). Water soluble adjuvants can increase droplet size and reduce the percent of spray volume in small driftable particles. Water applied at 56 ml/min without adjuvants produce a VMD of 139 μm with 34% in small driftable particles. The addition of 0.75% StaPut or Chem-Trol increased the VMD to 277 μm or 240 μm respectively, while reducing the small droplets from 34% to 25%.

Similar results were achieved by SUNDARAM et al. (1992). The addition of Sta-Put caused increasing of VMD and NMD and decreasing of number of droplets/cm^2.

The droplet size is important for pesticide efficiency. Whereas the efficiency of the systemic herbicides were not influenced by different droplet spectra, the efficiency of the contact herbicides were influenced a lot (PROKOP, VEVERKA 2003). Similar results were found by fungicides application. The application of fungicides with a contact + systemic active substance or a contact active substance + Agrovital® were not influenced by the droplet size, the application of the contact substance only influenced the efficiency a lot (PROKOP et al. 2003).

The experiments with Agrovital® (96% pinolene) and Ekol® (90% raps fluid, 10% polyetoxyl esters) showed that these surfactants influenced the droplet spectrum in spraying. The addition of adjuvants increased the droplet size and decreased the percentage of small droplets. Most important is the decreasing of droplets under 75 μm which are the major contributor to off-target drift.

Table 6. Number and volume of droplets under 75 μm – Ekol

Nozzle	Number of droplets under 75 μm	(%)	Volume of droplets under 75 μm (mm^2/10^3)	(%)
015F110	1,136	55.55	55,470.82	2.82
03F110	884	44.20	51,472.75	1.01
05F110	494	24.70	27,312.49	0.11
LD015F110	776	33.35	40,445.07	0.68
LD03F110	882	44.10	37,546.49	0.35
LD05F110	681	34.05	36,575.87	0.21
DB015F120	505	25.25	15,332.59	0.07
DB03F120	643	32.15	105,167.00	0.07
DB05F120	964	48.20	26,330.62	0.03

The low-drift nozzles increased VMD and NMD and produced fewer volume of drift prone droplets than standard flat-fan nozzles. Differences were found between two kind of the low-drift nozzles too. The Drift-BETA nozzles produced larger droplets and fewer volume of spray in small driftable particles than the Lo-Drift nozzles.

References

BERGER P.D., BERGER C.H., 1993. Effect of surfactant type and order of addition on droplet size and dynamic interfacial properties. In: BERGER P.D., DEVISETTY B.N., HALL F.R.

(ed.), Pesticide Formulations and Application Systems. Am. Soc. Test. Mater. STP 1183, Philadelphia: 157–172.

BLAHOVEC J., ŘEZNÍČEK R., 1988. Zemědělská letadla. Praha, VŠZ: 180.

BOUSE L.F., KIRK I.W., BODE L.E., 1990. Effect of spray mixture on droplet size. Trans. Am. Soc. Agric. Eng., *33*: 783–788.

HANKS J.E., 1995. Effect of Drift Retardant Adjuvants on Spray Droplet Size of Water and Paraffinic Oil at Ultralow Volume. Weed Technol., *9*: 380–384.

HOLLAND J.M., JEPSON P.C., JONES E.C., TURNER C., 1997. A comparison of spinning disc atomisers and flat fan pressure nozzles in terms of pesticide deposition and biological efficacy within cereal crops. Crop Protec., *16*: 179–185.

LEFEBVRE A.H., 1993. Droplet Production. In: MATTHEWS G.A., HESLOP E.C. (ed.), Application Technology for Crop Protection. CAB International: 35–54.

METODIKA SRS pro zkoušky strojů na ochranu rostlin, 2000.

PROKOP M., VEVERKA K., 2003. Influence of droplet spectra on the efficiency of contact and systemic herbicides. Plant Soil Environ., *49*: 75–80.

PROKOP M., KEJKLÍČEK R., VEVERKA K., 2003. Influence of droplet size on efficiency of contact and contact + systemic fungicides. Plant Protect. Sci. (submitted).

REED J.P., HALL F.R., REICHARD D.L., 1990. Influence of Atomizers Upon Efficacy of Tridiphane plus Atrazine Applied Postemergence. Weed Technol., *4*: 92–96.

SUNDARAM A., SUNDARAM K.M.S., ROBINSON A.G., BEVERIDGE W.J.G., LEUNG J.W., 1992. Drop Size Spectra and Deposit from Aerial Spraying with and without a Polymeric Adjuvant. Amer. Society Agric. Engineers, *35*: 387–394.

TRUNEČKA K., 1992. Kvalita práce v ochraně rostlin a možnosti jejího zvyšování. [Dizertační práce.] Brno, VŠZ: 131.

TRUNEČKA K., 1996. Technika a metody v ochraně rostlin. Brno, MZLU: 124.

YAUN-HUIZHU, TU-YUQIN, LI-YUNFAN, HUANG-HONGYING, QI-SHUHUA, YAUN-HZ, TU-YQ, LI-YF, HUANG-HY, QI-SH, 1997. Primary study of droplet deposition and distribution on flight *Mithimna separata* (Walker). Acta Phytophyl. Sin., *24*: 367–370.

Received 18 March 2002

Vliv pomocných látek na velikost kapek postřikového spektra

ABSTRAKT: Byl sledován vliv adjuvantů (Ekol® – 90 % řepkový olej, 10 % polyetoxylované estery a Agrovital® – 96 % pinolene) na utváření charakteristik kapkového spektra. Pro získání kapkových spekter byly využity dva typy nízkoúletových trysek LURMARK a standardní štěrbinové trysky LURMARK. Jako aplikační kapalina byla použita čistá voda a následně voda s adjuvanty (Agrovital v dávce 3 ml/10 l vody a Ekol v dávce 150 ml/10 l vody). Pro každé kapkové spektrum byl zjištěn střední objemový průměr (VMD), střední početní průměr (NMD), hraniční objemové parametry ($D_{0,1}$ a $D_{0,9}$), relativní faktor rozpětí a poměr VMD/NMD. Oba typy nízkoúletových trysek zvýšily hodnoty VMD, NMD a vytvářely menší objemové procento kapek náchylných k úletu (do 75 µm). Jak Agrovital® (Miller Chemical and Fertilizer Corporation US), tak Ekol® (JIZA a spol. v.o.s., Česká republika) způsobily zvětšení velikosti kapek (VMD, NMD) a snižovaly procento kapek náchylných k úletu.

Klíčová slova: Agrovital; Ekol; postřik; trysky; úlet postřikové kapaliny; velikost kapek

Corresponding author:

Ing. MARTIN PROKOP, Státní rostlinolékařská správa, Zemědělská 1a, 613 00 Brno, Česká republika
tel.: + 420 545 137 034, fax: + 420 545 327 024, e-mail: martin.prokop@srs.cz

Starter solenoid and power contacts diagnostics

J. Pošta, R. Pavlíček, T. Hladík

Czech University of Agriculture, Prague, Czech Republic

ABSTRACT: Availability of the combustion engine machines depends on the starter reliability. Starter failures are often caused by gradual damage of its particular parts, this process can be monitored by means of diagnostics. In this paper the results of the starter solenoid and power contacts diagnostics verification are summarized.

Keywords: starter; voltage waveform; starter solenoid; power contacts

Starter failures sources are either mechanical or electrical. Wear, seizure or fractures of moving parts come under mechanical sources of failures, short or interrupted circuit and contact resistance increase come under the latter (Fajman, Ondráček 2001).

In the most frequently used starter design the pull-in solenoid is used for engaging the pinion. The pull-in solenoid is suitable for low armature travel and high pull-in force. The solenoid armature moves the engaging lever, which engages the pinion into the mesh with ring gear of the flywheel. After the pinion is entirely engaged the total accumulator voltage is applied to the starting electromotor (PAL Magneton). Fig. 1 shows the electrical scheme of the frequently used starter design.

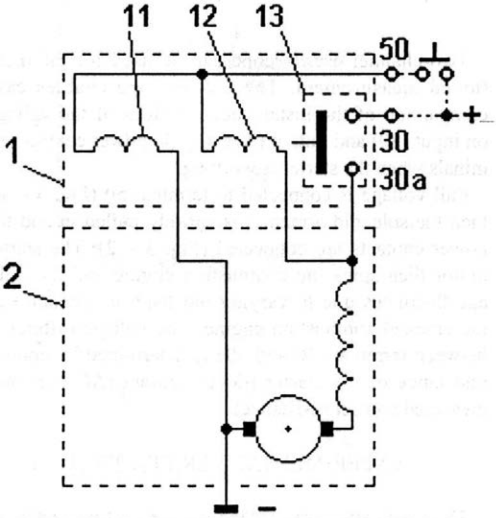

Fig. 1. Electrical scheme of the starter (Pavlíček 2001)
1 – pull-in solenoid
2 – electromotor
11,12 – solenoid hold-in and pull-in winding
13 – power contact
30 – power contact terminal
50 – solenoid terminal

MATERIALS AND METHODS

PULL-IN SOLENOID

The draw force of the solenoid (Pavlíček 2001) has the form

$$F = k \,.\, d \,.\, \mu_0 \,.\, \left(\frac{N \,.\, i}{2 \,.\, l}\right)^2 \qquad (1)$$

where: F – the draw force (N),
k – the armature length (m),
d – the armature diameter (m),
μ_0 – the vacuum permeability (H/m)
N – the solenoid winding number (1),
i – the instantaneous current (A),
l – the armature travel (m).

According to (1) it is obvious how the draw force is determined. The solenoid winding number N can change due to turn-to-turn winding fault, the drop of the instantaneous current i can emerge due to increased contact resistance. The draw force drops significantly in both mentioned cases. Considering the starter reliability, the starter end-of-life is reached when the draw force drops insofar it is unable to equal the passive resistance and the force of the solenoid armature pull-back spring.

Thus the solenoid armature draw force can be used as a diagnostic signal, which provides sufficient information on the character of the above mentioned factors and their variations in time. However, the draw force value is not measurable without disassembling. For practical use the draw force is thus not a suitable diagnostic signal.

The draw force value can be indicated indirectly by the solenoid armature pull-in time, or also by the time of engaging the pinion. The solenoid armature pull-in time can be obtained from uniformly accelerated motion formula, Newton's Second Law and equation (1). The substitution and rearrangement gives:

$$t = \frac{1}{N \cdot i} \cdot \sqrt{\frac{8 \cdot l^3 \cdot m}{k \cdot d \cdot \mu_2}} = \frac{1}{N \cdot i} \cdot c_s \qquad (2)$$

where: t – the solenoid armature pull-in time (s),
m – the armature and other parts mass (kg),
c_s – constant for given starter.

According to equation (2) the change of the solenoid winding number N (caused by turn-to-turn winding fault) and the drop of the instantaneous current i (caused by increased contact resistance) extends the solenoid armature pull-in time as a consequence of the armature draw force drop. Thus the solenoid armature pull-in time can be used as a diagnostic signal which provides sufficient information on the character of the above mentioned factors and their variations in time. The solenoid armature pull-in time can be easily measured without disassembling the starter by analyzing the terminal 50 voltage waveform using oscilloscope.

Full voltage is connected to terminal 50 (Fig. 2 – 1), then the solenoid armature is entirely pulled-in (Fig. 2 – 2) and the power contact connects full voltage to the starter electromotor. The starter motor then spins the combustion engine and the voltage fluctuates due to varying mechanical resistance of the cranked combustion engine. The time delay between points 1 and 2 is represents the armature pull-in time. If the solenoid's N value decreases due to turn-to-turn winding fault or the instantaneous current i decreases due to increased contact resistance of

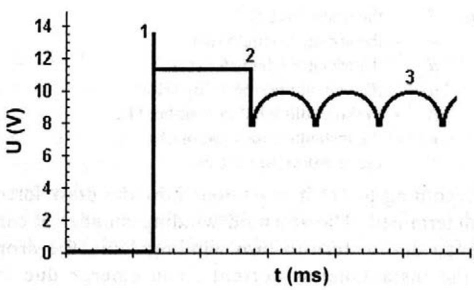

Fig. 2. Terminal 50 voltage waveform (PAVLÍČEK 2001)
1 – full voltage connected to terminal 50
2 – solenoid armature entirely pulled-in, power contacts connected
3 – starter electromotor working

the solenoid circuit, the pull-in time extends. Mentioned starter failures can be detected by comparing the voltage waveforms of faultless and tested starters.

STARTER POWER CONTACTS

During the combustion engine cranking process the starter electromotor circuit is carrying current of hundreds A. If the contact resistance of the power contacts increases, the losses increase and the starter output drops. The starter end-of-life is reached when the output is not sufficient for minimal cranking RPM of the combustion engine.

The contact resistance of the starter power contact is thus very important for reliable cranking.

The contact resistance is not easy to be measured directly (BALOG 1999).

Indirect measurement of the contact resistance is possible by measuring the power contact voltage drop. Effective values of the measured voltage are not suitable because of varying circumstances of the circuit; instantaneous values have to be measured instead (POŠTA, PAVLÍČEK 2002).

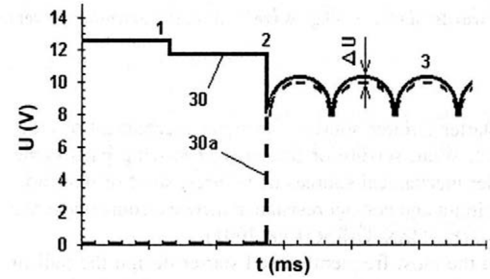

Fig. 3. Power contact terminals voltage waveform (PAVLÍČEK 2001)
1 – full voltage connected
2 – solenoid armature entirely pulled-in, power contacts connected
3 – starter electromotor working
30 – terminal 30 voltage
30a – terminal 30a voltage
ΔU – power contact voltage drop

Two-channel oscilloscope can be used for the mentioned measurement. The oscilloscope enables easy comparison of the instantaneous values of the voltage on input (30) and output (30a, Fig. 1) power contact terminals when the starter is working.

Full voltage is connected to terminal 50 (Fig. 3 – 1), then the solenoid armature is entirely pulled-in and the power contacts are connected (Fig. 3 – 2). The starter motor then spins the combustion engine and the voltage fluctuates due to varying mechanical resistance of the cranked combustion engine. The voltage difference between terminals 30 and 30a is determined by contact resistance of the starter power contact (ΔU indicates measured contact resistance).

EXPERIMENTAL VERIFICATION

The verification was carried out for starting system of Škoda Felicia 1.3:

- 4-cylinder combustion engine, 4-cycle, compression pressure 1.2 MPa, 124 teeth flywheel gear ring.
- Starter 12 V, 0.8 kW, type number 443 115 142 350, 9 teeth pinion, commutator diameter 35 mm, 28 commutator bars.
- Accumulator 12 V, 44 Ah, no-load voltage 12.8 V.

Table 1. Solenoid measurement results

Solenoid	Circuit resistance increase	Armature pull-in time	Terminal 50 voltage
	ΔR (Ω)	t (ms)	U (V)
Faultless	0	25	11.0
Increased resistance	0.2	50	8.5
Increased resistance	0.5	75	7.0
Increased resistance	1.0	∞	6.5

VERIFICATION OF THE PULL-IN SOLENOID DIAGNOSTICS

The instantaneous value of the voltage on terminal 50 was measured using digital oscilloscope (sample rate 4.883 kHz), realized by personal computer oscilloscopic converting card PCX-1230. The measurement was carried out for faultless starter and for starters with increased solenoid circuit resistance (PAVLÍČEK 2001). The results are summarized in Table 1 and Fig. 4.

VERIFICATION OF THE POWER CONTACTS DIAGNOSTICS

The instantaneous values of the voltage on terminals 30 and 30a were measured using digital oscilloscope with dual timebase (sample rate 4.883 kHz). The measurement was carried out for faultless starter and for starter with damaged power contacts (PAVLÍČEK 2001). The results are summarized in Fig. 5.

DISCUSSION

The solenoid armature pull-in time can be easily obtained from oscillogram of the terminal 50 voltage waveform. This time is proportional to the distance between first two peaks of the waveform.

Besides that, the oscillogram provides the information on the voltage drop (or the voltage level after the drop). This information indicates the accumulator state or short circuit failure of the solenoid circuit.

The voltage drop ΔU can be easily obtained from oscillogram of the terminals 30 and 30a voltage waveforms. From this the absolute and relative losses of the cranking output can be determined. In case 5A the losses amount to 50 VA if the current is 100 A (i.e. 5% considering common 12 V starting system). In case 5B and current 100 A the losses amount to 220 VA (i.e. 22% considering common 12 V starting system). This dissipated energy turns in heat which additionally strains the power contacts.

CONCLUSION

The experiments prove that the solenoid armature pull-in time is suitable technical state indicator for solenoid diagnostics. The pull-in time can be easily ob-

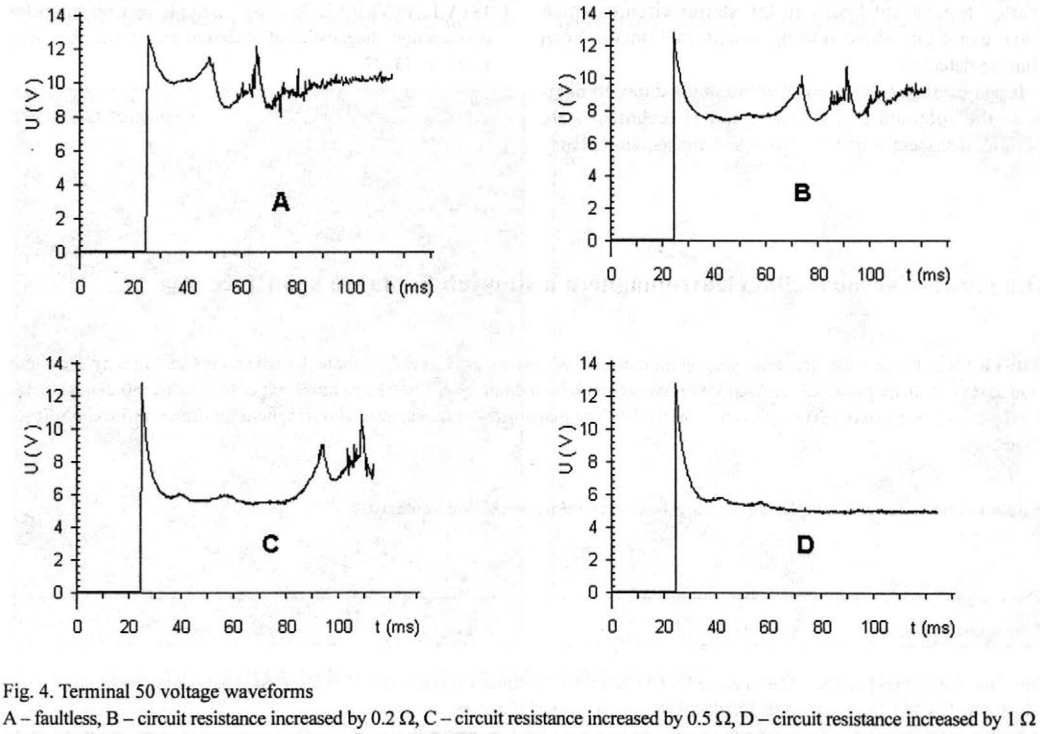

Fig. 4. Terminal 50 voltage waveforms

A – faultless, B – circuit resistance increased by 0.2 Ω, C – circuit resistance increased by 0.5 Ω, D – circuit resistance increased by 1 Ω

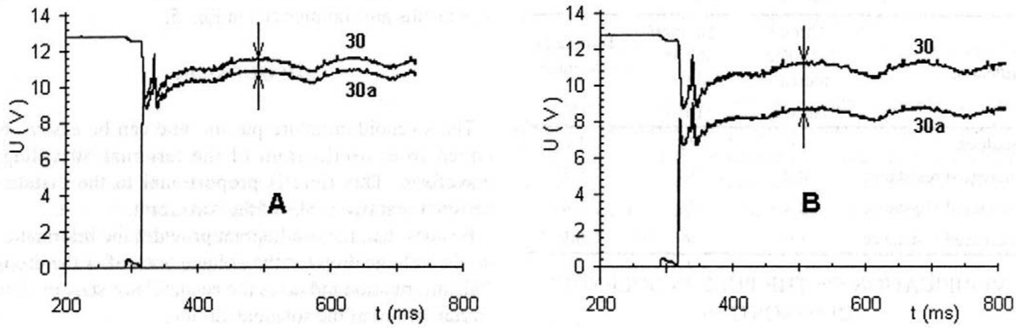

Fig. 5. Power contacts terminal voltage waveform
A – faultless, $\Delta U = 0.5$ V, B – damaged contact, $\Delta U = 2.2$ V

tained from the terminal 50 voltage oscillogram without disassembling the starter itself. The pull-in time sufficiently indicates the starter technical state reacting to the circuit resistance increase (possibly caused by increased contact resistance) as well as to the circuit resistance decrease (possibly caused by turn-to-turn winding fault). In both cases the solenoid armature pull-in time extends making it impossible to distinguish between these two cases, however the solenoid removal and its detailed inspection is necessary in both cases.

The experiments also prove that dual measuring of the power contact terminals voltage enables to diagnose increased contact resistance without disassembling the starter. Significant losses in the starter circuit (which often cause the whole starting system malfunction) can thus be detected.

It can be stated that described methods allow to diagnose the solenoid and power contacts technical state without disassembling the starter and consequently carry out decisions on its preventive renewal. This significantly contributes to availability of the whole machine.

References

BALOG J., 1999. Počítačová podpora diagnostiky traktorového motora. [Habilitačná práca.] Nitra, SPU: 198.

FAJMAN M., ONDRÁČEK J., 2001. A proposal for evaluating the operating state of agricultural tractors. Res. Agr. Eng., *47*: 27–32.

PAL Magneton, 2001. http://www.magneton.cz.

PAVLÍČEK R., 2001. Dynamická diagnostická měření. [Dizertační práce.] Praha, ČZU, TF: 114.

POŠTA J., PAVLÍČEK R., 2002. Sample rate selection for oscilloscopic diagnostics of alternator and starter. Res. Agr. Eng., *48*: 73–77.

Received 22 January 2002

Diagnostika zasouvacího elektromagnetu a silových kontaktů spouštěče

ABSTRAKT: Pohotovost strojů se spalovacím motorem do značné míry závisí na spolehlivosti spouštěče. Poruchy spouštěče jsou často působeny postupně narůstajícím poškozením jeho jednotlivých částí, které může být dobře sledováno diagnosticky. V příspěvku jsou shrnuty výsledky ověření osciloskopické diagnostiky zasouvacího elektromagnetu spouštěče a silového spínače spouštěče.

Klíčová slova: spouštěč; průběh napětí; zasouvací elektromagnet; silové kontakty

Corresponding author:

Doc. Ing. JOSEF POŠTA, CSc., Česká zemědělská univerzita, Technická fakulta, 165 21 Praha 6-Suchdol, Česká republika
tel.: + 420 224 383 266, fax: + 420 220 921 361, e-mail: posta@tf.czu.cz

SHORT NOTE

Vertical and horizontal distribution of pesticide microcapsules applied on the porous surface

R. AULICKÝ, V. STEJSKAL

Research Institute of Crop Production, Prague, Czech Republic

ABSTRACT: In microencapsulated pesticide formulations the active ingredient is concentrated into plastic microcapsules. After a spray application, these microcapsules do not spread uniformely on the treated surface. In wet droplets, most of microcapsules are evenly distributed while in the dry droplets the microcapsules form aggregations. This note reports that the degree of microcapsules aggregation in dry droplets depends on the surface texture. Rough and porous surfaces decrease aggregation of microcapsules in two ways: either by decreasing the horizontal "aggregative" movement of microcapsules or by increasing the vertical movement of microcapsules. The vertical movement of microencapsules leads to their submersion into the porous surface and consequently to the decrease of the bio-availability of encapsulated pesticide, which is lower on the paper than on the glass.

Keywords: pesticides; encapsulation; spatial distribution; surface texture

In microencapsulated pesticides (SC) the active ingredient (e.g. fenitrothion) is concentrated into plastic microcapsules (TSUDA et al. 1987). After the application of the water based spraying liquid, these microcapsules do not spread on the treated surface uniformely. The distribution pattern of pesticide deposits on the treated area influences the efficiency of a particular pesticide treatment (COURSHEE 1991a,b; EBERT, HALL 1999; EBERT et al. 1999). Most of the studies, while discussing various aspects of droplet distribution in detail, do not consider micro-distribution of active ingredient inside of single droplets. In the previous paper (STEJSKAL, AULICKÝ 2002) we described the "effect of intra-droplet aggregation" (Fig. 1) of insecticide microcapsules after

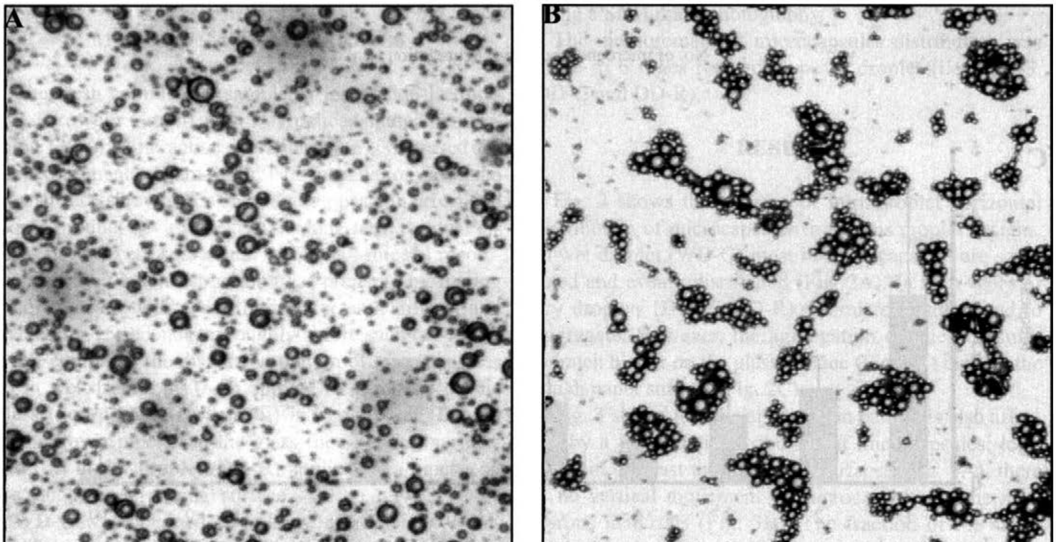

Fig. 1. Various degree of aggregation of microcapsules in wet (A), and (B) dry droplet

This work was supported by Grant of the Ministry of Agriculture of the Czech Republic No. M01-01-03.

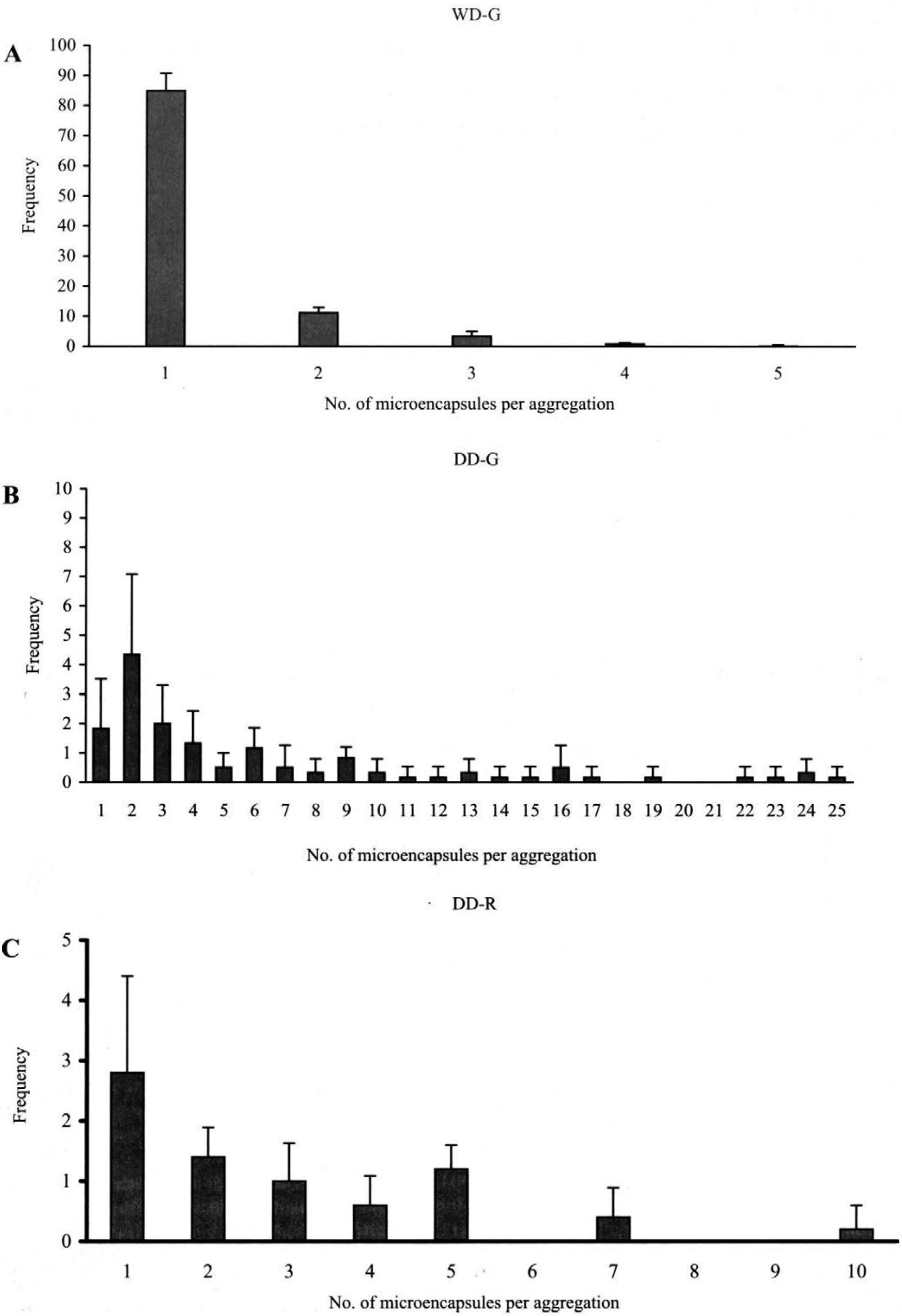

Fig. 2. Frequency of aggregations of microcapsules in: A – wet droplet applied on the non-porous glass surface (WD-G), B – dry droplet applied on the glass non-porous surface (DD-G), and C – dry droplet applied on the porous rough-paper surface (DD-R)

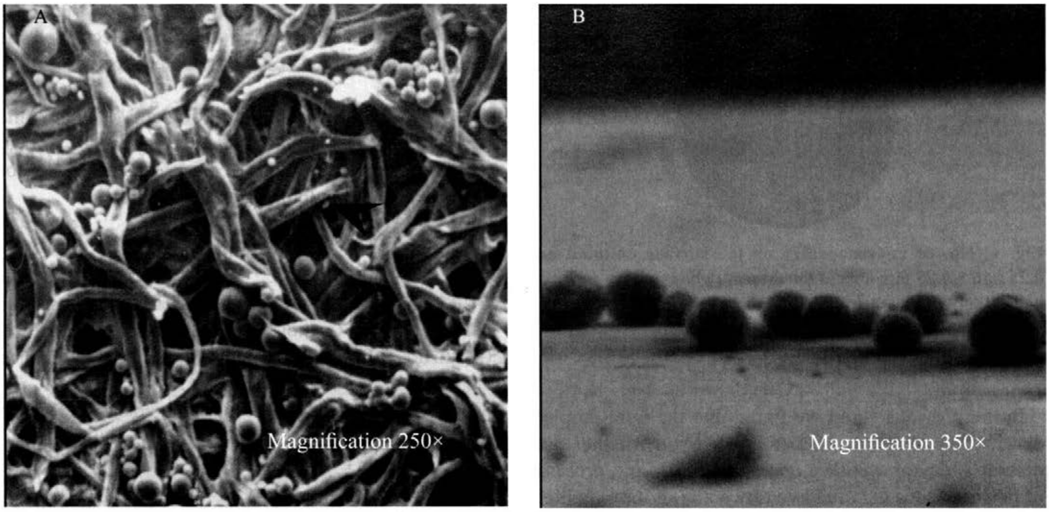

Fig. 3. Microcapsules on (A) porous paper surface, and (B) non-porous glass surface

their spray application, and discussed the implications of the "effect" for SC-pesticide efficiency. We found that in the wet droplets, most of microcapsules were separated and evenly distributed in the space while in dry droplets the microcapsules formed aggregations. However, the distribution of pesticide deposits was studied only when applied on the non-porous surfaces. Therefore, the aim of this complementary study was to compare the aggregative behaviour of pesticide microcapsules (Detmol-mic, a.i. fenitrothion) inside of droplet deposits on the porous and non-porous surfaces.

METHODS AND MATERIALS

The fresh commercial sample of insecticide Detmol-mic (Frowein Gmbh) with microencapsulated fenitrothion (20%) as an active ingredient (a.i.), was used for the experiments. Detmol-mic is a formulation designed as a surface spray to control crawling pests in urban and stored product environment by its long-term residual effect. Two percent spray fluid of Detmol-mic, as recommended by a label instruction, was prepared by mixing a concentrate with a distilled water as a diluent and shaken for 15 seconds thoroughly before each test.

We compared the dispersion pattern of microcapsules (i) in wet droplet **(WD-G)** applied by a pipette on the glass (non-porous) surface (ii) in dry droplet **(DD-G)** applied by a pipette on the glass (non-porous) surface, and (iii) in dry droplet **(DD-R)** applied by a pipette on the rough paper (porous) surface.

WD-G was obtained as follows: a droplet (0.04 ml) of 2% spray fluid of Detmol-mic was applied by a micro-pipette on the surface of the microscopic slide. The slide with a droplet was immediately put under a microscope at magnification 75× and photographed by a digital camera. The dispersion pattern was established from the photographs on 0.25 mm × 0.25 mm area of the droplet.

DD-G was obtained as in WD-G, but before counting microcapsules, the droplet was left dry for 2 hours at 20°C.

DD-R was obtained as in DD-G with the exception that the droplets were applied on the thick layer of the rough paper: one layer consisted from 5 pieces of filter paper Whatman No. 6. After application the filter paper with droplets was left dry as in DD-G and after that the pattern of microcapsules aggregation was estimated by using a SEM microphotography.

The measurement of microcapsules distribution was made in 6 times for each type of droplet (i.e. WD-G, DD-G and DD-R).

RESULTS

Fig. 2 shows the patterns of intra-droplet horizontal distribution of microcapsules in various droplet designs. In wet droplet (WD-G) most of microcapsules are separated and evenly distributed (Fig. 2A). In both types of dry droplets (DD-G, DD-R) the microcapsules tend to aggregate. However, the aggregation of microcapsules is much higher on the glass surface (Fig. 2B) than on the rough paper surface (Fig. 2C).

Fig. 3 shows that the aggregation pattern is also affected by a horizontal distribution of microcapsules: logically, in contrast to the porous surfaces (Fig. 3A), there is no vertical movement of microcapsules in the non-porous materials (Fig. 3B). The fraction of the smallest microcapsules tends to submerge into the internal structure of the porous material (e.g. Fig. 3A – black arrow). Fig. 4 demostrates that the surface bio-availability of microcapsules was lower on the porous rough paper (25%) than on the non-porous glass (100%).

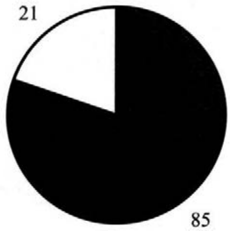

Fig. 4. No. of microcapsules on the surface counted on 0.25 mm × 0.25 mm area of the droplet (white: porous surface, black: non-porous surface)

DISCUSSION

In the previous study we found that the intra-droplet distribution of microcapsules depends on whether the droplet is dry or wet. We observed that drying process of droplet deposits is followed by a strong intra-droplet aggregation of microcapsules (Fig. 1B). In this consequent study we discovered that the degree of surface aggregation of microcapsules was also dependent on the type and texture of the surface receiving the encapsulated pesticide. Two processes were responsible for the final pattern of distribution of microcapsules on the porous surface. First, the complex inner structure of porous surface (Fig. 3A) decreased the horizontal (i.e. 2-dimensional) "aggregative" movement of microcapsules. Second, the porous structure also increased the "anti-aggregative" vertical (i.e. 3-dimensional) movement of microcapsules. The vertical movement was connected with a submersion of microcapsules into the porous paper material, which inherently decreased the bio-availability (Fig. 4) of encapsulated pesticide to the crawling pests.

We can conclude that while testing and modelling the activity of encapsulated pesticides, the effects of vertical and horizontal arrangement of microcapsules inside of droplet deposits should be taken into account.

References

COURSHEE R.J., 1991a. Pesticide efficiency and distribution – Part 1. Int. Pest Control., *44*: 89–93.

COURSHEE R.J., 1991b. Pesticide efficiency and distribution – Part 2. Int. Pest Control., *44*: 122–131.

EBERT T.A., HALL F.R., 1999. Deposit structure effects on insecticide bioassays. J. Econ. Entomol., *92*: 1007–1013.

EBERT T.A., TAYLOR R., DOWNER R., HALL F.R., 1999. Deposit structure and efficacy of pesticide application. 1. Interactions between deposit size, toxicant concentration and deposit number. Pest Sci., *55*: 783–792.

STEJSKAL V., AULICKÝ R., 2002. Uneven distribution of fenitrothion microcapsules (Detmol-mic) inside droplet deposits. Res. Agr. Eng., *48*: 36–40.

TSUDA S., OHTSUBO T., KAWADA H., MANABE Y., KISHIBUCHI N., SHINJO G., TSUJI K., 1987. A way of action of the fenitrothion microcapsule as a residual cockroach control formulation. J. Pestic. Sci., *12*: 23–27.

Received 28 May 2002

Vertikální a horizontální distribuce pesticidních mikrokapsulí aplikovaných na porézní substrát

ABSTRAKT: V mikroenkapsulovaných formulacích pesticidů (SC-pesticidy) není aktivní látka rovnoměrně rozptýlena v emulzi, ale koncentrována do plastových mikrokapsulí. V postřikové jíše a mokrých kapénkách jsou mikrokapsule rozptýleny rovnoměrně, zatímco v uschlých kapénkách dochází k jejich agregaci. Tato práce však ukázala, že stupeň agregace mikrokapsulí v suchých kapénkách závisí na textuře povrchu. Existují dva mechanismy, které vedou ke snížení agregeace mikrokapsulí na hrubém a porézním povrchu: porézní struktura omezuje horizontální pohyb mikrokapsulí a umožňuje vertikální pohyb mikrokapsulí. Vertikální pohyb vede k zanoření mikrokapsulí do vnitřní struktury porézního materiálu; tím je snížena jeho biologická dostupnost pro lezoucí škůdce ve srovnání s neporézním skleněným povrchem.

Klíčová slova: pesticidy; enkapsulace; distribuce kapének; kvalita povrchu

Corresponding author:

Ing. VÁCLAV STEJSKAL, Ph.D., Výzkumný ústav rostlinné výroby, Drnovská 507, 161 06 Praha 6-Ruzyně, Česká republika
tel.: + 420 233 022 217, fax: + 420 233 310 636, e-mail: stejskal@vurv.cz

INFORMATION

Method of calculation and heat exchange in air heliocollectors

L. I. ŽMAKIN, I. P. KORNJUCHIN

Moscow State Textile University, Moscow, Russia

Energy saving problem in southern regions of eastern Europe countries including Russia has gained a great importance. One of directions of this problem solution is the solar energy employment as a source of low potential heat. For realization it is necessary to implement working up new radioactive convective heat exchangers (solar collectors) with optimal technical and economic characteristics as well as development of technical methods of calculation. Analysis has shown the present time solar collectors from polymeric materials, air heating tubing devices particularly, have the best future. In the simple case these collectors can be made from two strips of polymeric foil (translucent and black) which are welded together on the sides and produce long cylindrical channel. Air heating takes a place at the air moving through this channel.

There is presented a method of heat exchange for this purpose. There were determined: 1. optical characteristics (coefficients of absorption and reflection) of translucent channel part considering multiple reflection of solar radiation in the foil; 2. temperature fields in channel cross section; 3. change of air heating mean temperature along channel length.

It is necessary to know the refractive index and absorption coefficient of radiation in polymeric foil for determination of optical characteristics of solar collector channel translucent wall. Refractive index was experimentally determined as ratio of foil actual thickness to optical one, it was $n = 1.26 \pm 0.02$. Weakening coefficient $k_з$ measured in experiments was appointed according to Buger law at normal ray incidence

$$I/I_0 = \exp(-k_з\delta) \qquad (1)$$

where: I_0, I – values of impeding and transmitted radiation intensities properly,
δ – foil thickness.

Weakening coefficient takes into account reflection and refraction of rays. For absorption actual coefficient determination by method of multiple reflection, the D foil absorption coefficient, for example, of non-polar radiation normal incidence was calculated.

$$D = \frac{d^2 \exp(-k\delta)}{1 - r^2 \exp(-2k\delta)};\; r = \frac{(n-1)^2}{(n+1)^2};\; d = \frac{4n}{(n+1)^2} \qquad (2)$$

where: r and d – reflecting and transmitting properties of air-foil surface,
k – actual absorption.

If we compare D and I/I_0 values calculated according to (1) and (2) equations we will have non-linear equation solution of which will give us absorption actual coefficient $k = 668$ l/m.

Foil transmittance and reflection properties were calculated in the range of $0 \leq \alpha \geq \pi/2$ incidence angles in accordance with Fresnel and Snellius formula taking into account polarization of non-polarized falling wave at reflection and refraction. Since the foil thickness is very small in comparison of soil collector channel radius, its curvature effect on rays reflection and refraction regularities was not taken into consideration.

Formulates for calculation of normal and tangential components of coefficients of transmittance D_n, D_t, absorption A_n, A_t and reflection R_n, R_t were obtained by the method of multiple reflections. Their formulae are

$$D_n = \frac{d_n^2 \exp(-k\frac{\delta}{\cos \beta})}{1 - r_n^2 \exp(-2k\frac{\delta}{\cos \beta})};\quad D_t = \frac{d_t^2 \exp(-k\frac{\delta}{\cos \beta})}{1 - r_t^2 \exp(-2k\frac{\delta}{\cos \beta})}$$

$$A_n = \frac{d_n\,[1 - \exp(-k\frac{\delta}{\cos \beta})]}{1 - r_n \exp(-k\frac{\delta}{\cos \beta})};\quad A_t = \frac{d_t\,[1 - \exp(-k\frac{\delta}{\cos \beta})]}{1 - r_t \exp(-k\frac{\delta}{\cos \beta})}$$

$$R_n = 1 - D_n - A_n; \qquad R_t = 1 - D_t - A_t$$

$$r_n = \frac{\sin^2(\alpha - \beta)}{\sin^2(\alpha + \beta)};\; r_t = \frac{\mathrm{tg}^2(\alpha - \beta)}{\mathrm{tg}^2(\alpha + \beta)};\; d_n = 1 - r_n;\; d_t = 1 - r_t$$

where: α – angle of incidence,
β – angle of refraction.

If we take into account that incidencing radiation is not polarized, total absorption, refraction and transmittance capacity of foil is possible to be presented as

$$A = 0.5\,(A_n + A_t); \quad R = 0.5\,(R_n + R_t); \quad D = 0.5\,(D_n + D_t)$$

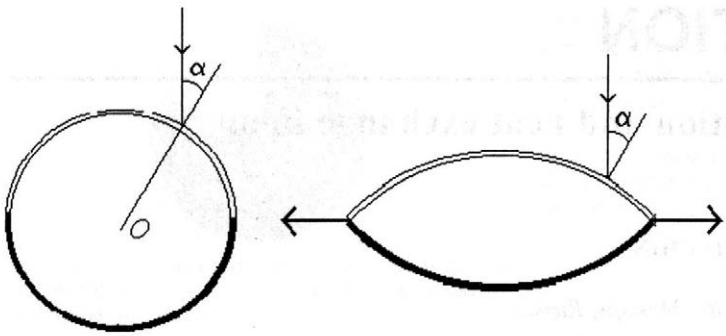

Fig. 1. Shapes of collector channels cross section

Data analysis calculated according to these equations allowed to determine an optimal form of cross section of tubing collector channel. Energy loss for this form is minimal. Since the collector channel has to be extended in cross section direction for this cross section formation with central angle which is equated to Bruster's dual angle (Fig. 1).

Radiation energy flow density absorbed with collector different walls was calculated for a round shape channel. This value for channel semi-transparent and non-transparent walls was determined according to

$$q_s = q_0 \varepsilon \cos \beta; \quad q_s = q_0 D \cos \beta \qquad (3)$$

where: q_0 – flow density of energy impinging of radiation energy collector, semi-transparent wall blackness degree ε is received as equal to its absorption ability.

Value q_s is presented in the graph (Fig. 2) for q_o = 500 W/m^2 dependent on central angle $\varphi = \pi/2$ counted off low formating wall of cylinder. As it would be expected the energy smallest absorption is occurring around central angle $\varphi = \pi/2$. In consequence of symmetry of studied problem involving horizontal surface, the graph is limited with values of angles $\varphi \leq \pi$.

It was considered at air temperature calculation in the channel that tubing collector was placed in unlimited air volume with the steady temperature t_o. Temperature fields in the channel was calculated with assistance of equation of energy for stabilized heat change at air laminar flow. In this case energy equation changes into thermal conductivity equation:

$$\frac{1}{r}\frac{\partial}{\partial r}(r\frac{\partial t}{\partial r}) + \frac{1}{r^2}\frac{\partial^2 t}{\partial r^2} = 0 \qquad (4)$$

where: r – radial co-ordinate,
t – temperature.

However the limiting conditions for this equation are difficult enough. First of all, it has be taken into account the dependence on angle co-ordinate density of flow absorbed in transparent and non-transparent walls of inside source radiation channel, this density having been calculated formerly (Fig. 2). Secondly, if channel walls have a different temperature, has to be taken into account a radiation heat exchange within them (over-radiation

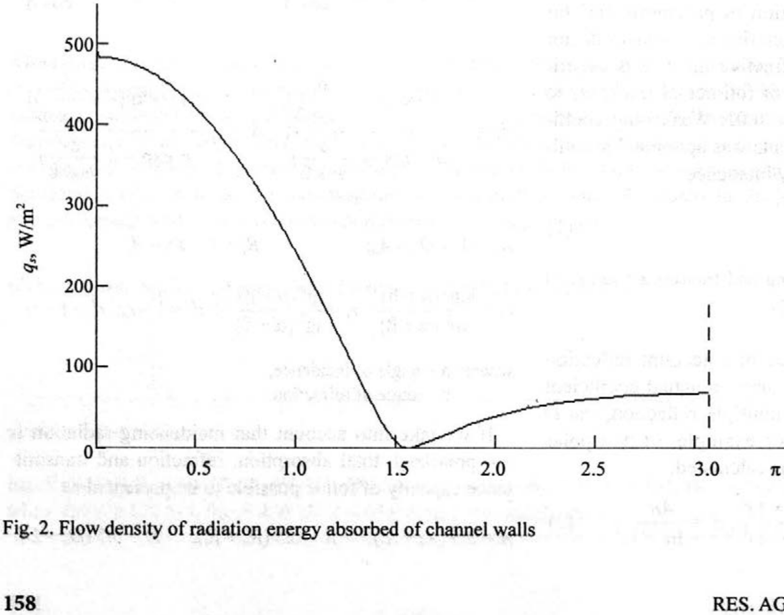

Fig. 2. Flow density of radiation energy absorbed of channel walls

of energy). In the end, it needs to take into account collector walls heat exchange with environment by way of convection and radiation.

Limiting conditions for (4) could be written as

$$-\lambda \frac{\partial t}{\partial r}\bigg|_{r=R} = q_c + q_{ro} + q_{ri} + q_{rr} - q_s \qquad (5)$$

where: q_s – density of flow of inside radiation absorbed,
q_c – convective,
q_{ro} – radiation heat losses into environment from outer surface of channel,
q_{ri} – heat radiation losses into environment from inside surface of channel through transparent foil,
q_{rr} – heat flow density due to over-radiation.

Heat losses were calculated in accordance with formulae:

$$q_{rr} = \sigma \int_0^{\infty}\int_0^{2\pi} \frac{1}{\frac{1}{\varepsilon}+\frac{1}{\varepsilon'}-1} \frac{T^4-(T')^4}{\pi} \frac{\sin^4 \frac{\varphi-\varphi'}{2}}{[\sin^2 \frac{\varphi-\varphi'}{2} + (X')^2]^2} dX' d\varphi'$$

$$q_{ro} = \int_0^{\pi/2} \sigma\varepsilon\, (T^4 - T^4_0) \sin 2ß dß; \qquad q_c = \alpha_c\, (t - t_o);$$

$$q_{ri} = \sigma \int_0^{\infty}\int_0^{2\pi} D\varepsilon \frac{T^4-T^4_0}{\pi} \frac{\sin^4 \frac{\varphi-\varphi'}{2}}{[\sin^2 \frac{\varphi-\varphi'}{2} + (X')^2]^2} dX' d\varphi'$$

$$X = x/2R; \qquad X' = x'/2R; \qquad L = l/2R$$

X and R are conformably to co-ordinate axes and channel radius; degree of channel non-transparent part – equal to incidence angle of absorption ability. Parameters without of top dash index belong to specific point of channel surface, heat losses are calculated for this point, parameters with pointed out indicated index – to other points of this surface. For q_{ri} calculation, a model was used with adjoining cover which had blackness degree of 1 and temperature of the environment. It allowed to employ the same attitude as in the over-radiation calculation; the only difference was in foil transmittance ability record.

It follows from equation (5) that limiting conditions are non-linear because of radioactive components. Since this problem has to be solved by iterative methods. Limiting conditions (5) were transformed for iterations convergence improvement. The mean coefficient was introduced for this heat transmission. It allowed for over-radiation and determined losses into environment

$$\bar{\alpha} = \frac{\bar{q}}{\bar{\vartheta}} \qquad (6)$$

where: $\bar{\vartheta}$ – mean temperature pressure and heat flow mean density were determined as mean integral on the channel surface

$$\bar{\vartheta} = \frac{1}{\pi}\int_0^{\pi} (t_{r=R}| - t_0)\, d\varphi; \quad \bar{q} = \frac{1}{\pi}\int_0^{\pi} [q_c + q_{ro} + q_{ri} + q_{rr}]\, d\varphi \qquad (7)$$

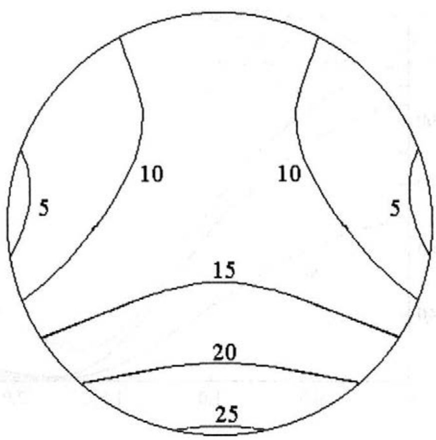

Fig. 3. Isothermal curve for excessive temperature of air in channel

In this case limiting conditions (5) are transformed to shape

$$-\lambda \frac{\partial \vartheta}{\partial r}\bigg|_{r=R} = \bar{\alpha}\vartheta + \delta q \qquad (8)$$

where $\delta q = q_{ro} - q_{ri} + q_{rr} + (\alpha_c - \bar{\alpha})(t|_{r=R} - t_0) - q_s$ is presented as function of central angle φ.

The equation (4) inscribed for excessive temperature ($\vartheta = t - t_0$) was approached by Furie's method of variables distribution. Since the temperature field is not known at the beginning, the iterative method was used in solution process. The small temperature difference (to 0.1° C) in every points of 33 on the channel surface served as final indication of iterative process.

Excessive a air temperature isotherms in solar collector channel are shown in Fig. 3, there is dependence of temperature losses due to convection and radiation from channel inside and outer surface in Fig. 4. It is evident from Fig. 3, heat losses are maximum in channel surface part limited with black foil. We emphasize the gained results belong to air stabilized flow which is proper to channel of theoretically endless length.

Approximate method of calculation of air mean temperature change along channel length was worked out. Radiation flow absorbed by collector can be divided on two parts – q_i transmitted into air and q_e drained into environment, that is

$$q = q_i + q_e = \alpha_i\, (t_w - t) + \alpha_e\, (t_w - t_0)$$

where: α_i, α_e – corresponding coefficients of heat transmission,
t, t_w, t_0 – air temperatures in channel, of channel wall and ambient air.

Temperature drop is following

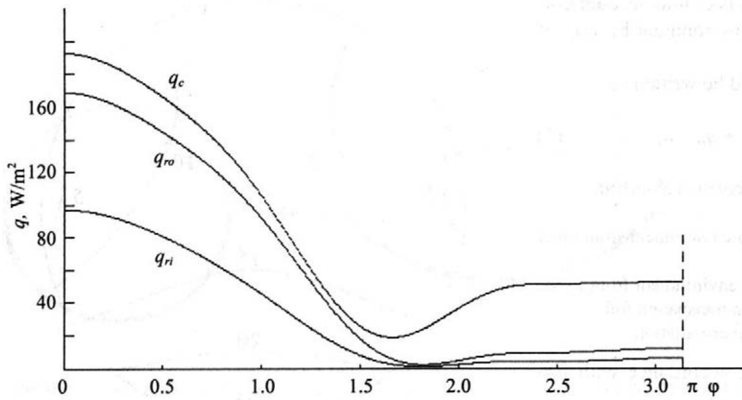

Fig. 4. Heat losses due to convection and radiation from outside and inside surface of channel

Temperature drop is following

$$t_w - t_0 = \frac{q + \alpha_i (t - t_0)}{\alpha_i + \alpha_e} = \frac{q + \alpha_i \vartheta}{\alpha_i + \alpha_e} \qquad (9)$$

Differential equation expressing air heating in the channel can be gained on the basis of heat balance for surface elementary part

$$\alpha_i (t_w - t)\, dF = c_p\, G dt \qquad (10)$$

where: G – rate of air flow.

According to (9) equation (10) is transforming to shape

$$\frac{K}{w} \cdot \frac{\alpha_i}{\alpha_i + \alpha_e} dX = \frac{d\vartheta}{q - \alpha_e \vartheta} \qquad (11)$$

where: $X = x/D$ – dimensionless axial co-ordinate of channel,
$K = 4/(\rho c_p)$,
ρ – air density,
w – air velocity,
D – channel diameter.

The equation (11) was integrated numerically with aid of Mathcad 6.0 programme at steady value of air velocity, under this condition air temperature on channel outlet as a function of Reynolds' number. Calculations were done for regime of flow around transition area from flow laminar regime to turbulent one. At this calculations, heat and hydrodynamical analogy take into account dependence of intermitted coefficient from co-ordinate and Reynolds' number. Calculation results were shown in Fig. 5. Presence of maximum on this dependence can be explained with flow turbulence occurrence and following this process heat transmission coefficient enlargement. The same maximum was observed in experiments.

"Long" channel concept is useful for practical application. Steady value of air temperature is determined in this "long" channel. This channel length is a relative value depending on air consumption and heat change conditions. Differential equation (11) was used to approach channels of different length, if temperature curve

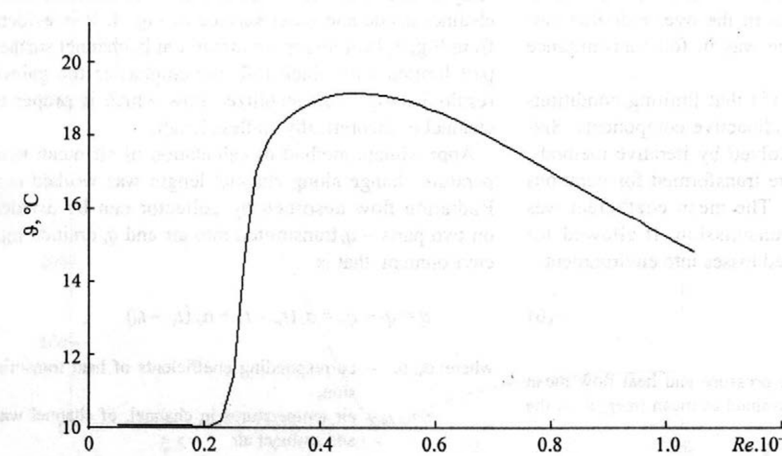

Fig. 5. Dependence of excessive temperature on output from channel with relative length $L = 175$ on Reynolds' number

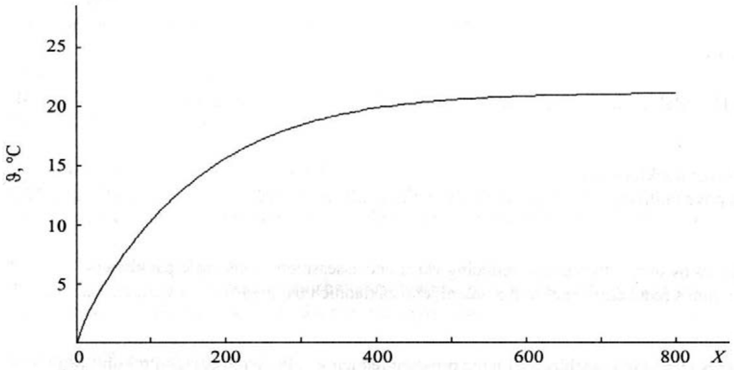

Fig. 6. Change of excessive temperature along channel length with relative length L = 800 at Re = 2,500

solution repeated. In Fig. 6 it is, for example, shown temperature curve for channel with relative length of 800. Temperature asymptotic value is gained in this channel. It is not really purposeful to choose a channel relative length more then 700, even though its final selection must be implemented on the basis of technical and economic calculations.

The presented methodology of heat calculation of tubing air solar collectors from polymeric materials can be applied at projection of the same devices characteristic compactness, transportability and enough effectiveness. Possible field of their application is air heating with solar energy for drying under field conditions, for example, of cotton, agricultural products and other materials.

Received 17 April 2001

Corresponding author:

Doc. Dr. LEONID IVAN ŽMAKIN, Moscow State Textile University, M. Kaluzhskaya 1, Moscow, 109456, Russia
tel.: + 7 095 171 19 20, fax: + 7 095 170 51 01, e-mail: energy@viesh.msk.su

INDEX OF VOLUME 48

REJSTŘÍK ROČNÍKU 48

INSTRUCTIONS FOR AUTHORS

The responsibility for the contents of a manuscript rests with the authors. The Editorial Board will decide on suitability for publication, after considering the scientific importance and overall technical quality of the manuscript and the comments of the referees.

The manuscript should be typed on standard A4 paper. A PC diskette with the complete text and including references, tables and figure legends of graphical documentation should be provided with each manuscript, indicating the used editor program.

Manuscript should consist of the following sections: Title page, Abstract, Keywords, Introduction, Materials and Methods, Results, Discussion, References, Address of corresponding author, Tables, Legends to figures.

The Title page must contain an informative title, complete name(s) of the author(s), the name(s) and address(es) of the institution(s) where the work was done.

The **Abstract** should state in a short and concise form what was done and how, and should contain basic numerical and statistical data representative of the results. It should be submitted in English and, if possible, also in Czech.

Keywords follow the abstract; they are ranked from general to specific terms, and are written in lower case letters and separated by semicolons.

The **Introduction** (without a subtitle) should consist of a short review of literature relevant to and important for the study. The reason(s) for carrying out the work may be included.

In **Materials and Methods**, the description of experimental procedures should be sufficient to allow replication. Abbreviations can be used if necessary; first use of an abbreviation should be just after its complete name or description. The International System of Units (SI) and their abbreviations should be used.

Results should be presented clearly and concisely.

The **Discussion** should interpret the results, without unnecessary repetition. Sometimes it is possible or advantageous to combine Results and Discussion in one section.

If **Acknowledgments** are needed, they come next.

References used in the text consist of author's name and year of publication. If there are more than two authors, only the first is named, followed by the phrase *et al.* The list of references should include only publications quoted in the text. These should be in alphabetical order under the first author's name, citing all authors, year (in brackets), full title of the article, abbreviation of the periodical, volume number, first and last page numbers.

Contact address should include the postal address, telephone, fax and e-mail numbers of the corresponding author.

Tables and Figures shall be enclosed separately. Each of them must be referred to in the text. Figures should be restricted to material essential for documentation and understanding of the text. Duplicate presentation of data in both tables and figures is not acceptable. All illustrative material must be of publishable quality. Both line drawings and photographs are referred to as figures. Photographs should have high contrast. Each figure should be accompanied by a concise, descriptive legend.

Reprint: Ten (10) reprints of each published paper are supplied free of charge.

POKYNY PRO AUTORY

Autor je plně odpovědný za původnost práce a za její věcnou i formální správnost. O uveřejnění práce rozhoduje redakční rada se zřetelem k lektorským posudkům, vědeckému významu a přínosu i kvalitě práce.

Rukopis musí být zaslán vytištěný na papíru formátu A4. K rukopisu je vhodné přiložit disketu s textem práce, popř. grafickou dokumentací pořízenou na PC (uvést použitý program).

Vědecké práce musí mít toto členění: titulní strana, abstrakt a klíčová slova, úvod, materiál a metody, výsledky, diskuse, literatura, kontaktní adresa, tabulky a obrázky včetně popisů.

Titulní strana musí obsahovat název práce, plné jméno autorů, název a adresu instituce, kde byla práce dělána.

Souhrn musí vyjádřit všechno podstatné, co je obsaženo ve vědecké práci, má obsahovat základní číselné údaje včetně statistických hodnot. Je uveřejňován a měl by být autory dodán v angličtině a češtině.

Klíčová slova (keywords, index terms) se připojují po vynechání řádku pod souhrn. Řadí se směrem od obecných výrazů ke speciálním; začínají malým písmenem a oddělují se středníkem.

Úvod (bez nadpisu) by měl obsahovat krátký přehled důležité literatury vztahující se k tématu a cíl práce.

Materiál a metody: Model pokusu musí být popsán podrobně a výstižně. Popis metod by měl umožnit, aby kdokoli z odborníků mohl práci opakovat. Zkratky jsou používány jen pokud je to nutné; první použití zkratky musí být uvedeno úplným popisem nebo vysvětlením. Používané měrové jednotky musí odpovídat soustavě měrových jednotek SI.

Výsledky: Doporučuje se nepoužívat k vyjádření kvantitativních hodnot tabulek, ale dát přednost grafům, anebo tabulky shrnout v statistickém hodnocení naměřených hodnot. Tato část práce by neměla obsahovat teoretické závěry ani dedukce, ale pouze faktické nálezy.

Diskuse obsahuje zhodnocení práce. Je přípustné spojení s předchozí kapitolou (Výsledky a diskuse).

Poděkování se uvádí před přehled použité literatury.

Literatura: Měly by být citovány práce uveřejněné v lektorovaných periodikách. V části Literatura se uvádějí jen práce citované v textu. Odkazy na literaturu v textu se provádějí uvedením jména autora a roku vydání publikace. Citace se řadí abecedně podle jména prvního autora: příjmení, zkratka jména, rok vydání (v závorce), plný název práce, úřední zkratka časopisu, ročník, první–poslední stránka; u knih je uvedeno místo vydání a vydavatel.

Kontaktní adresa obsahuje vedle poštovní adresy také čísla telefonu, faxu a e-mail autora pověřeného korespondencí.

Tabulky a obrázky: Tabulky, obrázky a fotografie se dodávají zvlášť a všechny musí být citovány v práci. Akceptovány budou pouze obrázky, které jsou nezbytné pro dokumentaci výsledků a umožňují pochopení textu. Není přípustné dokumentovat výsledky jak v tabulkách, tak pomocí grafů. Všechny ilustrativní materiály musí mít kvalitu vhodnou pro tisk. Fotografie i grafy jsou v textu uváděny jako obrázky a musí být průběžně číslovány. Každý obrázek musí mít stručný a výstižný popis.

Separáty: Autor obdrží 10 separátních výtisků publikované práce.

RESEARCH IN AGRICULTURAL ENGINEERING

Volume 48, No. 4 **2002**

CONTENTS

OBSAH

Vědecký časopis RESEARCH IN AGRICULTURAL ENGINEERING (Zemědělská technika) • Vydává Česká akademie zemědělských věd – Ústav zemědělských a potravinářských informací • Redakce: Slezská 7, 120 56 Praha 2, tel.: + 420 227 010 355, fax: + 420 227 010 116, e-mail: forest@uzpi.cz • Předáno do tisku 9. 12. 2002 •

Rozšiřuje Ústav zemědělských a potravinářských informací, Slezská 7, 120 56 Praha 2, tel.: + 420 227 010 427, e-mail: redakce@uzpi.cz